PENDING - Lender

Per

41301298

4/8/08

Bound

General Record Information

Request Identifier: 41301298 **Status:** PENDING 20080401
Request Date: 20080328 **Source:** ILLiad
OCLC Number: 7531052
Borrower: IDL **Need Before:** 20080407
Receive Date: **Renewal Request:**
Due Date: **New Due Date:**
Lenders: IAX, *JNA, UIU, HL8, GZH
Request Type: Copy

Bibliographic Information

Call Number:
Title: Molecular physiology.
ISSN: 0166-3178
Imprint: [Amsterdam] : Elsevier/North-Holland, c1981-c1985.
Article: Rae JL and Levis RA: Patch voltage clamp of lens epithelial cells: Theory and practice.
Volume: 6
Date: 1984
Pages: 115-162
Verified: <TN:60109> OCLC

My Library's Holdings Information

LHR Summary: 1-8(1981-1985)
Lending Policies: Unknown / Unknown
Location: JNAA
Copy: 1
Call Number: PERIODICAL HARD COPY
Format: unspecified

Borrowing Information

Patron: Eisenberg, Robert
Ship To: ILL/Rush University Library/600 S. Paulina/Chicago, IL 60612
Bill To: same
Ship Via: ARIEL
Electronic Delivery:
Maximum Cost: IFM - $50.00
Copyright Compliance: CCL
Email: ARIEL: ariel.rush.edu
Borrowing Notes: WE WILL ACCEPT INVOICES IF NO IFM

Molecular Physiology, 6 (1984) 115–162
Elsevier
MPH 267

PATCH VOLTAGE CLAMP OF LENS EPITHELIAL CELLS: THEORY AND PRACTICE

JAMES L. RAE and RICHARD A. LEVIS

Rush Medical College, Departments of Physiology, and Ophthalmology 1750 W. Harrison Street, Chicago, Illinois 60612, U.S.A.

(Received 14 November 1983, accepted 14 December 1983)

Key words: Current flow; Ion channel; Ion transport; Lens epithelium; Voltage clamp

Summary

The technique of patch voltage clamping has allowed us to resolve the current flowing through a variety of individual ionic channels in the apical membrane of the lens epithelium of several species. We have analyzed and produced electronics which have resulted in improved signal-to-noise ratios for single channel recordings and we have studied several glasses which provide lower noise level recording and/or improved sealability to lens membranes. We describe the procedures which we have implemented which permit single channel recordings to be made routinely from our epithelial cells. The advantages and disadvantages of inside-out, outside-out, on-cell, and whole cell recording are also presented. Time records and current-voltage data from several different kinds of epithelial ionic channels are provided. We discuss both strengths and limitations of current patch clamp techniques and places where we believe improvements are necessary.

Introduction

It is now known that current flow through biological membranes often occurs by the movement of ions through specific membrane proteins called channels. These channel proteins are able to assume one or more conformations in which a fluid-lined pore joins the inside of the cell with its bathing solution; it is through these pores that ions move. The role of such ionic channels in epithelial tissues has by necessity been investigated using indirect methods such as short circuit current and/or intracellular voltage determinations following ionic substitutions in the bathing solution. More recently, fluctuation analysis across epithelia, which measures the ensemble behavior of many of these channels acting together, has shown quite convincingly that epithelia have ionic channels similar to those identified in other membranes (Lindemann and Van Driessche, 1977; Van Driessche and Zeiske, 1980a,b; Lindemann, 1980; Zeiske

0166-3178/84/$03.00

and Van Driessche, 1981). In the next few years, much additional progress can be anticipated in the characterization of epithelial ionic channels because of the advent of the patch voltage clamp (Neher et al., 1978; Neher, 1981; Hamill et al., 1981). In this technique, a fire polished glass electrode which is connected to a sensitive current-to-voltage converter is pressed against the cell membrane and suction is applied until a high resistance seal occurs between the pipette and cell (Fig. 1). A small patch of membrane is thereby isolated and the currents which flow through single ionic channels are resolved. Because it is often possible to isolate the membrane patches from known regions of the cell and to control the electrochemical gradient across the membrane patch, both the spatial location and the selectivity of the ionic channels can be determined.

The advantages of measuring from small numbers of channels in isolated membrane patches have been known for some time. Over the past few years, there have been several strategies for the isolation of membrane patches (Neher and Lux, 1969; Fishman, 1973; Conti and Neher, 1980). Until recently, the seal or shunt resistance between the patch pipette and membrane was limited to the range of megohms which allowed the observation of some single channels with a rather poor signal to noise ratio (Neher and Sakmann, 1976; Neher and Steinbach, 1978; Nelson and Sachs, 1979; Jackson and Lecar, 1979). The important recent advance resulted from the observation that firepolished, clean electrodes in contact with cell membranes often produced seal resistances of many gigohms when suction was applied (Neher, 1981).

To date using these techniques, single ionic channel recordings have been reported from nerve (Lux et al., 1981; Yellen, 1982; Brown et al., 1982; Sigelbaum et al., 1982), cardiac muscle (Colquhoun et al., 1981; Reuter et al., 1982; Cachelin et al., 1983), skeletal muscle (Sigworth and Neher, 1980; Horn and Patlak, 1980; Horn et al., 1981a,b; Hamill and Sakmann, 1981; Pallotta et al., 1981; Auerbach and Sachs, 1983; Blatz and Magleby, 1983), egg cells (Fukushima, 1981, 1982), chromaffin cells (Marty, 1981; Fenwick et al., 1982a,b), photoreceptors (Bacigalupo and Lisman, 1983), a few epithelial type cells (Maruyama and Petersen, 1982; Maruyama, et al., 1983; Sauve et al., 1983) and others.

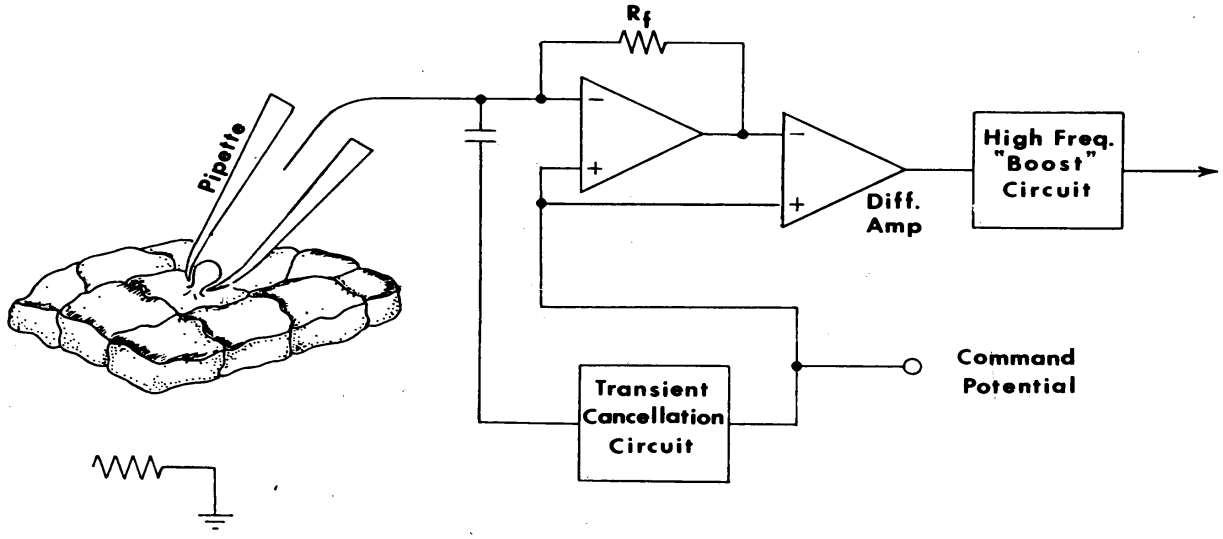

Fig. 1. Schematic representation of a patch voltage clamp recording configuration.

We have spent the last year applying this technique to the epithelium of the lens. During that time, currents from single ionic channels in a few thousand membrane patches have been observed. It is the purpose of this review to present a summary of our experience with patch clamping of lens epithelium and to present both a practical and theoretical description of the patch clamp technique. We have organized the content into 5 sections. The first is Patch Clamp Electronics. This is a detailed discussion of the dynamic and noise performance of the patch clamp. It describes sources of noise and ways to implement circuitry to minimize the noise and support the widest bandwidth of recording possible with present technology. The second section, Patch Clamp Methods, describes glasses useful for patch clamping and detailed procedures for pulling, coating, polishing, and filling the electrodes. It further describes how to produce gigohm seals and how to design a set up for patch clamping intact epithelia. The third section, Patch Clamp Configurations, describes different ways in which the membrane patch can be isolated and discusses the strengths and weaknesses of each. In addition, the method for voltage clamping entire cells through the patch electrode is described. This section concludes with a somewhat speculative analysis describing how the whole cell clamp configuration might be used for measuring the kinetics of ion pumps. The fourth section, Lens Epithelial Channels, briefly describes 11 different kinds of channels which have been seen in the apical membrane of the lens epithelium from 6 different species of animals. Time records and current–voltage relationships are presented for the various channel types. The final section, Perspectives, deals with places where improvements in the patch clamp are needed. In addition, the usefulness of the technique with possible pitfalls is discussed. It is our intention that within these 5 sections, there will be useful information both to the newcomer to patch clamping and to those already skilled in its use.

We will not cite all references where the patch clamp technique has been used. Since this technique is one of the newest and most exciting to biophysicists, the number of publications in which it has been used is proliferating at a rapid rate. There has already been a review of the technique (Hamill et al., 1981) and there is, in press, an entire book dealing with the details of the method (Sakmann and Neher, 1983). Therefore, we will simply refer to these sources for areas in which we have no special contributions. From the onset, we know that our contribution will have limitations. There are simply parts of the technique in which we have limited experience. For example, we have not applied the technique of whole cell clamping to our epithelial preparations and thus have little to contribute in this area. Also, for reasons we will discuss later, analysis of channel time records in our epithelia is presently at a rudimentary level and thus we refer to the work of others for a discussion of single channel analysis (Colquhoun and Hawkes, 1977, 1978, 1982; Horn and Lange, 1983; Sachs et al., 1983; Dionne et al., 1982; Fitzhugh, 1983; Horn, 1984).

PATCH CLAMP ELECTRONICS

Dynamic performance

The dynamic performance of a patch voltage clamp has been discussed previously

by Levis (1981) and Hamill et al. (1981; see also Sigworth, 1983). We will focus our attention on several of the more important and practical points, with emphasis on those areas in which we believe we have made significant contributions.

Gain-bandwidth product

A large gain-bandwidth product (GBW) is required for the 'headstage' amplifier or current-to-voltage converter, as shown by the following simple analysis (Levis, 1981). The situation is depicted in Fig. 2; here the headstage amplifier is considered to be described by a single pole roll-off, i.e., the output voltage, V_o, is given by $V_o = A_0(V_+ - V_-)/(1 + s\tau_p)$, where V_+ is the voltage at the noninverting input of the headstage, V_- is the voltage at the inverting input, f_p is the frequency of the pole of the open loop gain of the headstage amplifier, $\tau_p = 1/2\pi f_p$, A_0 is its open DC loop gain, s is the Laplace transform variable, $s = j\omega$, $\omega = 2\pi f$, and C_{in} is the inherent input capacitance of the amplifier plus stray capacitance (see below) at its inverting input. From Fig. 2 it can readily be derived that:

$$V_o \sim \frac{i_m R_f}{1 + s\tau_f + s^2\tau_u\tau_{in}} \quad \text{for } \tau_f >> \tau_f,\ \tau_{in} >> \tau_f. \tag{1}$$

where $\tau_f = R_f C_{if}$, $\tau_{in} = R_f C_{in}$, $\tau_u = \tau_p/A_0$; Note that $\tau_u = 1/2\pi f_u$, where f_u is the open loop unity gain frequency of the amplifier. If it is assumed that $R_f = 50\ G\Omega$, $C_f = 0.02$ pF, and $C_{in} = 20$ pF, such that $\tau_f = 10^{-3}$ s and $\tau_{in} = 1$ s, then for $f_u \leq 640$ kHz, equation (1) has a complex conjugate pair of poles with a natural frequency, f_n, given by $1/[2\pi(\tau_u\tau_{in})^{1/2}]$, and a damping coefficient (Clark, 1964) given by $\tau_f/]2(\tau_u\tau_{in})^{1/2}]$. In this situation the response to a square pulse o of current will ring, and simple 'booste circuits of the type considered below (see also Hamill et al., 1981; Levis, 1981) will be

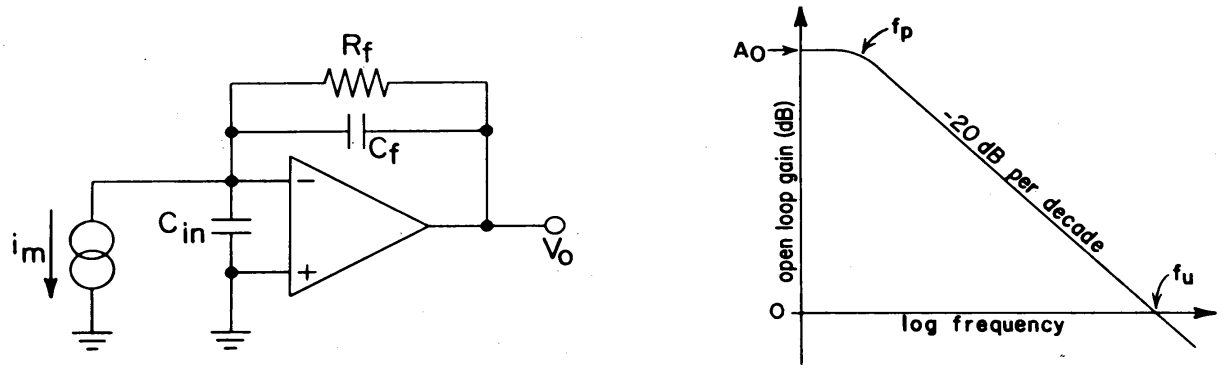

Fig. 2. At left: simplified equivalent circuit of the patch clamp current to voltage converter ('headstage'). C_{in} is the inherent input capacitance of the amplifier plus strays; R_f is the feedback resistor and C_f is the capacitance shunting R_f; i_m is the current from the patch membrane. At right the assumed form of the open loop gain of the headstage amplifier is illustrated as a function of frequency. As described in the text, the open loop frequency response of the amplifier is described by a DC gain A_0 that rolls-off at -20 dB per decade with increasing frequency as the result of a single pole located at f_p. The frequency at which the amplifier gain is one, is called f_u, the unity gain frequency.

inadequate to significantly extend the bandwidth of current measurement. For $f_u >$ 640 kHz, equation (1) has two real poles. As f_u increases, the frequency of the first pole approaches $1/2\pi\tau_f$ (159 Hz), and the secondary pole moves to progressively higher frequencies, approximated by $1/(2\pi\tau_u\tau_{in}/\tau_f)$. The frequency of the secondary pole represents the widest possible bandwidth of current measurement that is achievable with a boost circuit of the simple type described below, and is therefore of considerable importance to the practical use of the patch clamp.

At the time of this writing most headstage amplifiers are constructed from a discrete FET input stage followed by a low noise wideband operational amplifier (Levis, 1981; Hamill et al., 1981). As described below, amplifiers of this sort can readily have a gain-bandwidth product in excess of 100 MHz. It can be shown (Levis, 1981) that provided that the secondary pole in the open loop gain roll-off of the headstage amplifier is at a sufficiently high frequency, then an analysis that replaces the gain-bandwidth product of the headstage amplifier with an equivalent (one pole approximation) unity gain frequency will not be significantly in error. Commercially available operational amplifiers with sufficiently low input current noise to be used in the patch voltage clamp generally have unity gain bandwidths on the order of 1 MHz and should therefore be avoided for wideband (> 1 kHz) uses of the patch voltage clamp. As described below, 'composite amplifiers' with a discrete FET input stage also offer significantly less input voltage noise than commercially available op amps, and are therefore superior both in terms of noise and achievable bandwidth to any operational amplifier presently available.

High frequency 'boost' circuit

Feedback resistors with values sufficiently large for use in the patch voltage clamp have a frequency response that is inadequate to resolve fast openings and closings exhibited by most single channels. For example, a 50 GΩ resistor that is shunted by only 0.02 pF will exhibit an inherent time constant of 1 ms, which corresponds to a –3dB bandwidth of only 159 Hz. Regardless of the GBW of the amplifier employed, both the signal and the noise will be effectively passed through a 1 pole filter with this bandwidth (i.e., 159 Hz). There are only two solutions to this problem. One is to substantially increase the inherent frequency response of the feedback resistor, and the other is to use some form of analog or digital correction to restore the bandwidth (for both signal and noise) that has been lost due to the limited frequency response of the feedback resistor. Although the former alternative may seem attractive in principle, it is difficult to achieve in actual practice. The value of C_f mentioned above (0.02 pF) already approaches the minimum feasible for physically achievable resistors, and, with a 50 GΩ resistor, even a 10-fold further reduction in this capacitance would not be sufficient to produce reliable detection of single channel events of duration less than about 100–200 μs. Most resistors that are otherwise suitable for use as the feedback element in the patch voltage clamp have values of C_f in the range of 0.05–0.5 pF. Obviously, reducing the value of the feedback resistance (provided that the same shunt capacitance can be maintained) can extend the bandwidth of current measurement, but at the expense of signal to noise ratio (see discussion of feedback resistor noise below). It is now generally accepted that the most practical solution to the

problem of limited bandwidth arising from a large valued feedback resistor is to boost the high frequency response of the measurement with a subsequent analog circuit (Digital correction for the roll-off induced by the feedback resistor and headstage amplifier can be extremely accurate and essentially noise-free. However, to our knowledge this approach has not yet been implemented, and may not be practical without an array processor). The circuit that we use for this purpose is illustrated in Fig. 3. The performance of this circuit is most easily understood if amplifier A is initially considered in isolation. If this operational amplifier is considered to be ideal (i.e., infinite gain and bandwidth, Jung, 1980), then its transfer function is given by:

$$V_A = V_{in}(1+s(\tau_1+\tau_2))/(1+s\tau_2) \quad (2)$$

where the definitions of the τs and Vs are given in Fig. 3. The time constant τ_2 is used: (1) to prevent the circuit from oscillating (this function can also be served by a very small valued capacitor in parallel with R_1), and (2) to establish a high frequency roll-off to limit wideband noise. This latter function is best served by the use of a high order low pass filter (e.g., an 8 pole Bessel filter) with adjustable cut-off, but we have found that τ_2 is often necessary for stability (see below) and is convenient as a 'first-pass' at filtering the measured current. τ_1 is the more important time constant; it is a zero in the transfer function and can be used to cancel the first pole in the frequency response of the measured current directly at the headstage output (i.e., V_{in}). It is always intended in this circuit that $\tau_1 >> \tau_2$, so that $\tau_1+\tau_2 \approx \tau_1$, and the frequency of the zero can be set independently of that of the pole. The frequency response of the measured current directly at the headstage output can be described by $i_m R_f/(1+s\tau_f)$, provided that the amplifier has sufficiently large GBW and the resistor is adequately described by an ideal lumped resistance, R_f, in parallel with a lumped capacitance, C_f ($\tau_f = R_f C_f$). If the actual feedback resistor and headstage amplifier meet these criteria, then amplifier A of the boost circuit will be adequate by itself; i.e., the overall transfer function at the output of A will be given by $V_A = i_m R_f[1+s(\tau_1+\tau_2)]/[(1+s\tau_f)(1+s\tau_2)]$, so that if $\tau_1+\tau_2 = \tau_f$, $V_A = i_m R_f/(1+s\tau_2)$. Since τ_2 can be set to several 10 s of kHz (see below), the usable bandwidth can be increased by more than two orders of magnitude.

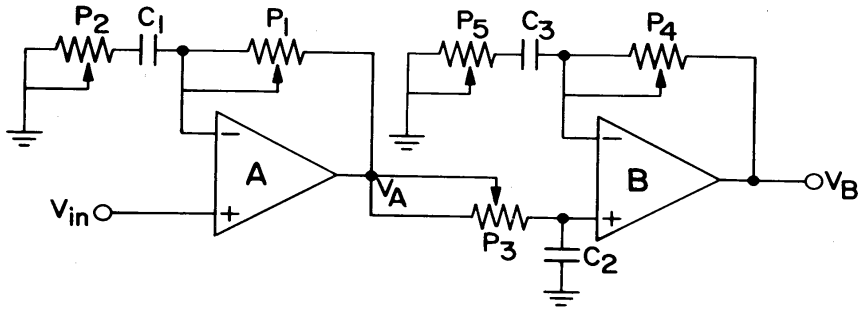

Fig. 3. High frequency 'boost' circuit used to increase the bandwidth of patch current measurement. If the settings (in ohms) of potentiometers P_1–P_5 are called R_1–R_5, respectively, then $\tau_1 = R_1C_1$, $\tau_2 = R_2C_1$, $\tau_3 = R_3C_2$, $\tau_4 = R_4C_3$, $\tau_5 = R_5C_3$. V_{in} is the output of the headstage amplifier following appropriate subtraction of the command voltage; V_A and V_B are the outputs of amplifiers A and B, respectively. We use and recommend Vishay (Malvern, PA) model 1202 trimming potentiometers for P_1–P_5.

Unfortunately, most high valued resistors are not adequately described by a lumped resistance in parallel with a pure lumped capacitance. Thus a simple boost circuit consisting only of amplifier A is not generally adequate to accurately restore the high frequency components of the measured patch current. We have found the two amplifier circuit illustrated to be adequate for several varieties of GΩ resistors; its complete transfer function, again assuming that amplifiers A and B have infinite gain and bandwidth, is given by:

$$V_B = V_{in} \left\{ \frac{[1+S(\tau_1+\tau_2)][1+S(\tau_4+\tau_5)]}{(1+s\tau_2)(1+s\tau_5)(1+s\tau_3)} \right\} \quad (3)$$

The transfer function has three poles and two zeros, the frequencies of which are all independently adjustable provided that $\tau_1 >> \tau_2$ and $\tau_4 >> \tau_5$. The time constant τ_5 serves the same purpose as τ_2 described above, and is only necessary for stabilization of amplifier B. Many high valued resistors when used in the feedback loop of the headstage produce a transfer function that is adequately described by $V_o = i_m R_f(1+s\tau_a)/[(1+s\tau_b)(1+s\tau_c)]$ (i.e., the roll-off of the impedance has two dispersions). For such a resistor the boost circuit should be adjusted such that $\tau_1+\tau_2 = \tau_b$, $\tau_4+\tau_5 = \tau_c$, and $\tau_3 = \tau_a$, so that $V_B = i_m R_f/(1+s\tau_2)(1+s\tau_5)$.

The above analysis implies that there is no limit to the ultimate bandwidth of current measurement achievable by the boost illustrated in Fig. 3. This, of course, is not the case. To illustrate the effects of the finite bandwidth of the operational amplifiers, the transfer function of amplifier A will again be considered in isolation, but the amplifier open loop gain will be assumed to roll-off at 20 dB per decade with increasing frequency (as assumed for equation 1). In this case:

$$V_A = \frac{V_{in}\{1+s(\tau_1+\tau_2)\}}{1+s(\tau_u+\tau_2) + s^2\tau_u(\tau_1+\tau_2)}$$

where $\tau_u = 1/2\pi f_u$ and f_u is the open-loop unity gain frequency of the amplifier. For a resistor with an un-boosted time constant (τ_f) of 1 ms, the value of $\tau_1+\tau_2$ ($\simeq \tau_1$) should be set to 1 ms, and with an amplifier with $f_u = 20$ MHz it will be found that the largest achievable natural frequency will be 56 kHz and that τ_2 must be set to about 6μs to achieve critical damping. This is more than adequate for any practical patch clamp measurement, but, for example, if τ_f (and therefore τ_1) were 10 ms and f_u were only 4 MHz, the natural frequency following boosting would be limited to a maximum of 8 kHz. Similar considerations apply to amplifier B. We have used OPA 101 s ($f_u \simeq 20$ MHz) from Burr-Brown (Tuscon, Arizona) as amplifiers A and B and have been able to boost the −3 dB bandwidth with a 50 GΩ resistor to about 30 kHz; and OP-27 (Precision Monolithics Inc., Santa Clara, CA) with $f_u \simeq 8$ MHz is adequate to achieve about 15 kHz. Boosting restores the high frequency components of both the signal and background noise. As described by Levis (1981) this can be accomplished without significantly increasing the noise above that which would have existed had the frequency response of the feedback resistor been infinite.

The scope of review does not permit detailed analysis of other aspects of the

dynamic performance of the overall patch clamp circuity, such as capacity transient cancellation and series resistance compensation (which is important for whole cell clamping). We refer the interested reader to Hamill et al. (1981), Levis (1981) and Sigworth (1983) for detailed discussions of these and other topics related to dynamic performance.

Practical design of an FET input 'headstage' amplifier

A practical design for a FET input headstage amplifier is illustrated in Fig. 4. $Q_{1A,B}$ are the two sides of a U430 dual JFET (Siliconix) which is used to form a differential preamplifier (input stage). A_1 is a commercial operational amplifier (OP27/37, Precision Monolithics Inc.) and forms the second high gain stage of the overall amplifier. $Q_{3A,B}$ is a 2SK240V dual JFET (Toshiba, Tokyo, Japan; U.S. distributor: Solid State Inc. Bloomfield, NJ) configured as a constant current source. $Q_{2A,B}$ is a 2SK240V operating as a pair of common-gate amplifiers; together with Q_1 they form a differential cascode amplifier (Evans, 1981). We operate the constant current source at 12 mA, i.e., 6 mA per side, and establish a drain-to-source voltage (V_{DS}) of about 3.5 V for the U430. The complete circuit is referred to as a 'composite amplifier'.

It is beyond the scope of this review to provide sufficient details of the theoretical and practical electronics required for the reader who is not familiar with transistor circuit design to thoroughly understand the operation of such a composite amplifier. However, several books and review articles may be consulted for further background information and details (Evans, 1981; Jung, 1980; Dostal, 1981; Netzer, 1981). Instead we will limit our discussion to certain critical features of the design and provide references as required where more basic details can be found.

Although the simpler current source shown in Fig. 4B of Hamill et al. (1981) is generally adequate for the patch clamp headstage and may be substituted for the current source in Fig. 3 without serious changes in performance, we prefer the circuit illustrated because of its higher output impedance and the 'second order' benefits this confers. Moreover, it is relatively simple and requires very little space to construct. Q_{3A} is the basic current source; the potentiometer P_1 is used to set the desired current level (here 12 mA). The required setting of P_1 can be determined from $V_{GS} = V_p[1-(I_D/I_{DSS})^2]$ where the 'pinch-off' voltage, V_p, is the value of V_{GS} for which the drain current, I_D, is zero; I_{DSS} is the drain saturation current, and I_D is the desired drain current; the desired setting of P_1 (the value of which, in ohms, will be called R_S) is then $R_S = V_{GS}/I_D$. For the 2SK240V, I_{DSS} ranges from 10 to 20 mA and V_p is typically about 0.7 V. As an example, for $I_{DSS} = 14$ mA and $V_p = 0.7$ V, $R_S = 15.5\ \Omega$ will produce the desired 12 mA current. The output conductance of Q_{3A} (i.e., $\delta I_D/\delta V_{D3A}$) is given by $g_{os}/(1+R_S g_{fs})$, where g_{os} is the inherent output conductance of the FET. The cascading of Q_{3A} by Q_{3B} (Evans, 1981, pp. 248–249) will greatly decrease the output conductance in terms of changes in the source voltage (V_{S1}) of the input transistor pair (i.e., $\delta I_D/\delta V_{S1}$). Resistors R_3 and R_4 set the voltage at the gate of Q_{3B} at a fixed level above the negative supply voltage (V_{s-}), and, provided that V_{s-} remains constant, this is equivalent to setting the gate of Q_{3B} at a fixed voltage above that of the source of Q_{3A}. In this case, for variations of V_{S1}, the overall output conductance ($\delta I_D/\delta V_{S1}$) is

$g_{os}^2/[g_{fs}(1+R_S g_{fs})]$, if it is assumed that g_{os} and g_{fs} are the same for both sides of Q_3. The overall output conductance can be as low as $3\text{–}5\times10^{-8}$ mho using the 2SK240V as shown; other dual JFETs can also be substituted for the 2SK240V, but will generally result in higher output conductances. Although the 2SK240V was selected primarily for its low g_{os} and large g_{fs} an additional benefit in the present situation is that 12 mA is very near I_{DZ} for this FET, i.e., the zero-temperature drift drain current (Evans, 1981, pp. 94–98), so that variations of I_D with ambient temperature will be minimized.

A simple common-source differential FET amplifier such as that used by Hamill et al. has a voltage gain of $g_{fs}R_D$. For the U430 operated at 6 mA per side g_{fs} is usually in the range of 12–16 mmho, and for $R_D = 1300\ \Omega$ (resulting in a 7.8 V drop across these resistors), this means that the differential gain of such an input stage will be 16–21. The cascode differential amplifier (Evans, 1981, pp. 77–83, 110–112; Netzer, 1981; Tobey et al., 1971, pp. 44–47) formed by $Q_{1A,B}$ and $Q_{2A,B}$ has essentially the same voltage gain as that of a simple common-source stage, and also reduces Miller effect input capacitance (Evans, 1981) and can therefore improve the dynamic performance of the composite amplifier. As illustrated, the gate voltages of $Q_{2A,B}$ are set at about +4.5 V; varying the ratio of R_1 and R_2 is a convenient method for setting the desired value of the drain-to-source (V_{DS}) of Q_1. For reasons that will be discussed below, we have chosen to operate Q_1 at $V_{DS} \simeq 3.5$ V. The cascode configuration can be shown not to significantly increase the equivalent input noise of the differential stage above that of Q_1, since any noise associated with Q_2 and R_1, R_2 is attenuated by g_{os1}/g_{fs1} ($\simeq 0.01\text{–}0.02$ for the U430 operated at $I_D = 6$ mA per side and $V_{DS} \simeq 4$ V) when referred to the input. Although the cascode configuration adds no appreciable noise to the circuit, we expect, and have verified experimentally, that it is not necessary for adequate noise performance in the patch clamp headstage; i.e., it does not substantially reduce the noise from that which results if a simple common-source differential stage is used. Its chief advantages are in terms of dynamic performance. In this regard, it can be noted that further reductions in input capacitance and increases in common mode rejection can be achieved by referencing the gates of $Q_{2A,B}$ to V_{S1}. One way of accomplishing this is to attach the grounded end of R_1 to the joined sources of $Q_{1A,B}$ (capacitor C_1 is eliminated) and to replace R_2 with a constant current source. If the current of such a source is called I_C, then $V_{G2A,B} = V_{S1} + I_C R_1$. However, in this case I_C must also be supplied by the current source formed by Q_3; in certain situations this is undesirable and can be overcome by placing a unity gain buffer amplifier (voltage follower) between V_{S1} and R_1. Although we have tried all of these configurations, we do not believe that the added complexity is justified in terms of improved performance and therefore recommend the simpler configuration illustrated.

We have used the U430 as the input FET for our headstages for more than two years (see Levis, 1981; Rae and Levis, 1983) and have consistently advocated it as the best selection for the input stage. All single channel records illustrated in this review were recorded with such a headstage. We selected the U430 for low noise for reasons that will be described below. In recent months (see Sigworth, 1983) it has become generally accepted that this dual JFET will provide the lowest noise of any that is presently commercially available when used as the input stage of a patch voltage clamp.

$R_{D1} = R_{D2}$ have been selected to be 1300 Ω so that the voltage at the drains of $Q_{2A,B}$

will be about +7 V, this provides an adequate drain-to-source voltage drop across Q_2 and a voltage gain for the input stage of about 20. Improved common mode rejection can be achieved by the use of a small (≈100 Ω) potentiometer, P_2, between the drain resistors as illustrated in Fig. 4. In general, however, this is not required, particularly if a reasonably low noise power supply is used. We use a battery supply (±19 V, nominal) regulated to ±15 V with home-made voltage regulators designed for stable output voltage and low noise (< 20 $nV/Hz^{1/2}$ at frequencies above ≈100 Hz).

Selection of the second stage operational amplifier, A_1, is based on its noise and bandwidth. It can easily be shown (see e.g., Motchenbacher and Fitchen, 1973) that, when referred to the input, to voltage noise of second stage operational amplifier A_1 is attenuated by the gain of the input stage (here ≈20). Thus, if the input voltage noise of the differential amplifier is 2 $nV/Hz^{1/2}$, the equivalent input voltage noise of the overall composite amplifier will be increased to only 2.06 $Nv/Hz^{1/2}$ if the input voltage noise of A_1 is 10 $nV/Hz^{1/2}$. We use an OP-27 (Precision Monolithics Inc.) for A_1 with e_n = 3 $nV/Hz^{1/2}$ (the input current noise of this op amp in conjunction with the drain resistors results in a negligible increase in the ineffective input voltage noise). The unity gain bandwidth of the OP 27 is 8 MHz, so that the overall gain-bandwidth product (GBW) of the composite amplifier can be as large as 160 MHz. With an OP-37

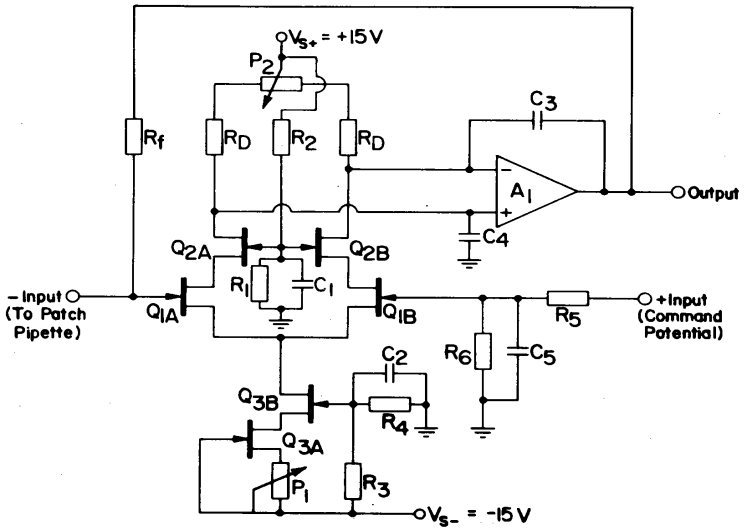

Fig. 4. Schematic diagram of a practical headstage amplifier design. Q_1 is a U430 (Siliconix) dual FET; Q_2 and Q_3 are 2SK240V (Toshiba) dual FETs. Other parameter values are as follows: $R_1 = 2\,k\Omega$, $R_2 = 5\,k\Omega$, $R_3 = 2\,k\Omega$, $R_4 = 2\,k\Omega$, $R_5 = 1.5\,k\Omega$, $R_6 = 50\,\Omega$, $R_D = 1.3\,k\Omega$, $R_f = 10$–$50\,G\Omega$, $C_1 = 47\,\mu F$, $C_2 = 47\,\mu F$, $C_5 = 0.02\,\mu F$. P_1 is a 50 Ω trimming potentiometer (Vishay model 1240W) and P_2 is a 100 Ω unit (Vishay model 1240 W). R_5 and R_6 form an attenuator (1/31) for the command input; i.e., a signal applied to the non-inverting input of the command amplifier must be 31 times the potential which is to appear at the pipette. Voltage noise in the command potential will form current noise in conjunction with any stray capacitance (C_s, see text) at the inverting input. R_5 and R_6 will attenuate any noise in the command potential 31-fold and only add the voltage noise of the 50 Ω resistor (0.9 $nV/Hz^{1/2}$); for a ±10 V signal source it allows the patch potential to be changed by up to ±320 mV. If appropriately implemented, noise in the command potential can also be effectively eliminated by means of the transient cancellation circuitry (see Hamill et al., 1981; Levis, 1981; Sigworth, 1983). The constant current source formed by $Q_{3A,B}$ is intended to deliver 12 mA, i.e., 6 mA per side of the U430. All resistors (except R_f) are metal film or bulk metal (Vishay) types; C_1 and C_2 are tantalum capacitors, C_5 is a ceramic capacitor, and C_3 and C_4 (if used) are silver mica capacitors.

(e_n = 3nV/Hz$^{1/2}$, GBW ≃ 40 MHz) the overall gain-bandwidth can be increased to roughly 1 GHz. Several other commercially available operational amplifiers can also serve as A_1 and provide entirely adequate performance, e.g., the NE5534 (Signetics) or OPA-101/102 (Burr-Brown). Capacitors C_3 and C_4 (note that C_3=C_4) are used to stabilize the overall composite amplifier when the feedback loop is closed without degrading noise performance. These capacitors are not generally necessary when the composite amplifier is used as a patch clamp current-to-voltage converter. However, if stability problems are encountered they can easily be eliminated (at the expense of open loop GBW) by using small valued silver-mica capacitors in these locations.

The selection of an appropriate GΩ feedback resistor is also very important to the overall performance of the headstage and will be discussed below. With a 50 GΩ chip resistor we have achieved the noise illustrated in curve a of Fig. 5 with a circuit that is generally similar to that illustrated in Fig. 4.

Noise performance

Noise in the current measured with the patch voltage clamp technique can be conveniently divided into three general catagories on the basis of its origin. These are: (1) electronic noise; (2) seal noise; (3) pipette noise.

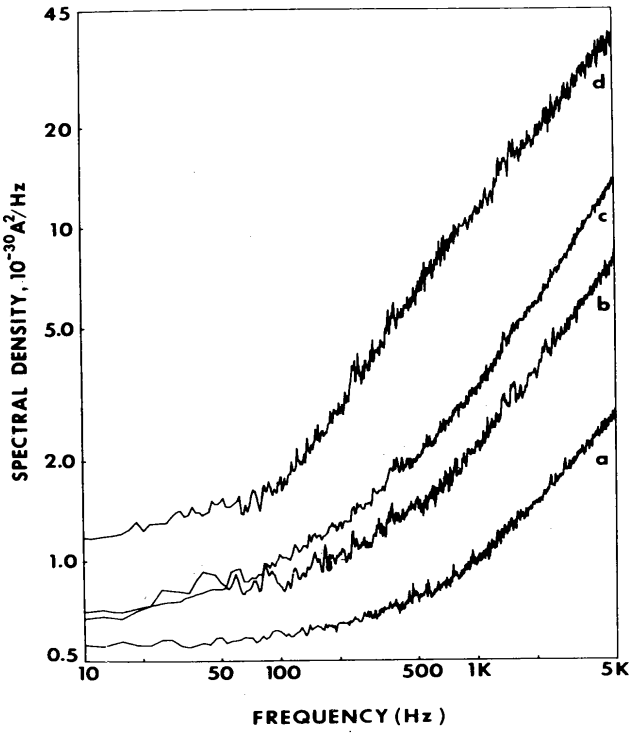

Fig. 5. Power-spectral density of the noise of the headstage alone (a) and the total noise with patch electrodes made from three different electrode glasses, Sylgard-coated, and sealed to Sylgard. Glasses are Corning #1723 (b), Corning #7052 (c), and Kimble #R-6 (d). Spectral densities at 5 kHz in units of 10^{-30} amp^2/Hz are: (A) = 2.6, (B) = 7.3, (C) = 13.7, (D) = 36.4. The curves were wild-point edited at multiples of 60 Hz. High resistance seals to lens membranes with these glasses frequently give noise levels comparable to those in the figure when no field exists across the patch.

1. *Electronic noise*

(A) Feedback resistor. The spectral density, S_f, of the thermal (Johnson) current noise arising from the feedback resistor of the headstage amplifier is given by:

$$S_f = 4kT\ Re\ \ Y_f \qquad \text{(units: Amp}^2\text{/Hz)} \tag{4}$$

Where k is Boltzman's constant, T is the absolute temperature (K), and $Re\ \{Y_f\}$ denotes the real part of the feedback resistor admittance. Equation (4) is a simple application of the Nyquist relationship, and in general is only expected to represent the total noise of the resistor when no net current flows through it. Ideally, the equivalent circuit of a physical resistor is just a resistance, R_f, in parallel with a small shunt capacitance, C_f. In this case, $Re\ \{Y_f\}$ is just $1/R_f$ and equation (4) becomes $S_f = 4kT/R_f$, and is independent of frequency. With the assumptions described above (see Fig. 2), the observable current noise spectral density directly at the output of the headstage amplifier ($S_{f,obs}$), will be shunted by the capacitance C_f such that:

$$S_{f,obs} = (4kT/R_f)/(1 + \omega^2 R_f^2 C_f^2)$$

where $\omega = 2\pi f$. The signal current is also filtered at precisely the same frequency as the noise. High frequency components of both the signal and noise can be restored by the boost circuit without significantly increasing noise above the level that would have existed in the absence of C_f, (i.e., $4kT/R_f$) (see Levis, 1981). In the rest of the discussion of noise performance, we will assume that the current is observed after appropriate 'boosting' of the feedback resistor frequency response.

Even an ideal resistor of the sort considered so far will also display excess noise when current passes through it (see e.g., Motchenbacher and Fitchen, 1973, pp. 171–179). This excess noise will have a spectral form that is approximately $1/f$. However, for high valued resistors such noise will rarely exceed the thermal noise floor at frequencies above about 1 Hz, and is thus of little practical importance.

Unfortunately, most high valued (i.e., GΩ range) resistors are not well described by a lumped resistance in parallel with a lumped capacitance. Instead, resistors of sufficiently high values to be used in the patch voltage clamp usually have a distributed shunt capacitance. If the capacitance is distributed evenly along the resistance, then no excess noise should result (the real part of the admittance is still $1/R_f$). However, if the capacitance is unevenly distributed then the real part of the admittance may readily exceed $1/R_f$ at moderate to high frequencies, and excess high frequency noise must be expected. This can easily be verified by consideration of a simple series combination of two parallel RCs ($R_1 \| C_1$ and $R_2 \| C_2$, with $R_f = R_1 + R_2$). In the extreme situation where $C_1 >> C_2$, the impedance of the resistor will decline from its low frequency value (R_f) to R_2 in the frequency range around $1/2\pi R_1 C_1$, and then finally decline toward zero at frequencies above $1/2\pi R_2 C_2$. The real part of its admittance, when referred to the input, will rise from $1/R_f$ to $1/R_2$. This situation is very much over-simplified, but represents the general behavior that can be expected from high valued resistors. For any particular resistor the magnitude of this effect must be assessed experimentally.

It is difficult to measure excess noise of this type, since an ideal feedback element would be required as a standard with which other resistors could be compared. In the absence of such an 'ideal' resistor, it is difficult to distinguish between the noise arising from the resistor and other noise sources. Thus, without rather difficult procedures such as using a capacitor as the feedback element to assess the noise of the headstage other than that of the resistor, about the best that can be done is to compare the noise of the same headstage with different resistor types. We have used this somewhat unsatisfactory procedure to assess several varieties of high valued resistors. It is our experience that chip resistors from National Micronetics (West Hurley, NY) are by far the best that have been available in recent years for the purposes of the patch voltage clamp. Unfortunately, at the time of this writing, these resistors are no longer commercially available; however, they are used in the EPC7 patch voltage clamp recently released by List Electronics (U.S. distributor: Medical Systems Corp., Great Neck, NY). We have found that Kobra resistors from K&M Electronics, Victoreen resistors (type MOX 750-24, suggested to us by W. Nonner), and type CX65 resistors from (Electronic GmbH, Unterhacting/Munich, F.R.G., no longer commercially available, but used in the EPC5 patch voltage clamp from List Electronics) all can be adequately 'boosted' by the circuit described above, but all possess significantly more excess high frequency noise than the National Micronetics product.

(B) *Headstage.* The special density, S_n, of the current noise arising from the 'headstage' amplifier or current to voltage converter is adequately described by:

$$S_n = 2qi_g + 4\pi^2(C_{gs} + C_s)^2 e_n^2 f^2 + S_c(f) \qquad \text{(units: Amp}^2\text{/Hz)} \tag{5}$$

Where q is the elementary charge (1.6×10^{-19} Coulomb), i_g is the gate operating current, C_{gs} is the gate-to-source capacitance of the input FET pair, C_s is any stray capacitance at the summing junction (inverting input) of the amplifier, e_n is its input voltage nose, f is the frequency in Hz, and S_c is a term arising from the packaging of the input FET that will be discussed below. The first two terms of equation (4) represent the 'ideal' or theoretically expected noise arising from the amplifier, while $S_c(f)$ is a 'non-ideal' term.

The term $2qi_g$ is the shot noise of the input gate current (Motchenbacher and Fitchen, 1973; Netzer, 1981). For $i_g = 1$ pA it amounts to 3.2×10^{-31} Amp^2/Hz, which is equivalent to the Johnson (thermal) noise of a 50 GΩ resistor. It is our experience that this expression quite adequately accounts for the low frequency current noise of the headstage in excess of that arising from the feedback resistor. The value of i_g depends on the particular FET selected for the amplifier input stage; it is however, fairly variable to any particular variety of FET and also depends on the drain to source voltage, V_{DS}, at which the FET pair is operated. For the U430, the value of i_g can range from less to 0.5 pA to more than 10 pA. Thus selection of an acceptable FET pair is important for 'home-made' patch clamp headstages. In the case of the U430 more than half of the 50 or so units we have tested have acceptable values of i_g (< 2 pA at 25°C) for all but the most demanding applications, provided that V_{DS} is set to be less than 4–5 V. Many other types of dual JFETs have sufficiently low values of i_g to serve as the input stage for the current to voltage converter (e.g., U421, U401, NDF9406,

2SK240), but are inferior to the U430 in terms of high frequency noise. For most JFETs i_g increases gradually as V_{DG} is increased until the i_g 'breakpoint' is reached; thereafter i_g becomes an exponential function of V_{DG}. For the U430 the i_g breakpoint occurs in the range of $V_{DG} = 4$–6 V, and we have therefore chosen to limit operating V_{DG} to less than 4 V. I_g breakpoint is also a function of drain current, I_D, such that it occurs at smaller values of V_{DG} as I_D increases. It should also be recognized that i_g is highly temperature-dependent, roughly doubling for each 10°C inrease in temperature. Thus for highly sensitive low frequency measurements a stable temperature must be maintained to avoid drift in i_g, and under some circumstances it may be desirable to select a FET with very small input gate current such as the U421. Small values of V_{DS}, already advocated to avoid operation beyond the i_g breakpoint, also serve to minimize self heating of the FET which can increase i_g.

The term $4\pi^2 e_n^2(C_{gs}+C_s)^2 f^2$ is the theoretically expected current noise arising from the input voltage noise, e_n, of the input FET pair (see Van der Ziel, 1963; Netzer, 1981) its input capacitance plus additional stray capacitance at the amplifier summing junction. Manufacturer's data sheets often show plots of e_n *vs* frequency for various values of drain current (I_D). Some manufacturers also show plots of equivalent input current noise, i_n, as a function of frequency, and these are typically shown to begin at a level determined by $2qi_g$, but rise at frequencies above 1–10 kHz. In this e_n–i_n convention it is usual to assign $i_n^2 = 2qi_g + 4\pi^2 e_n^2 C_{gs}^2 f^2$ (Netzer, 1981; Van der Ziel, 1962, 1963); this approach has often been used, but is generally inconvenient for describing the noise of the patch voltage clamp.

It is theoretically expected that the input voltage noise of a FET at moderate to high frequencies arises from the thermal noise of the FET channel and is given by $e_n^2 = 4kT\nu/g_{fs}$ (Van der Ziel, 1962; Netzer, 1981; Motchenbacher and Fitchen, 1973), where g_{fs} is the FET transconductance, and ν is a factor that is near unity. For the U430 operated at a drain current of 6mA per side, g_{fs} is roughly 15 mmho, so that values of e_n (for each side) as low as 1 nV/Hz$^{1/2}$ may be expected at frequencies in the kHz range. Actual measurements usually show somewhat more noise than this, but we have found that units can be selected with e_n as low as 1.3 nV/Hz$^{1/2}$ at 5 kHz. From equation (5), it can be seen that the best FET for low noise aplications should minimize the product $e_n C_{gs}$, or equivalently C_{gs}/g_{fs}. It was on this basis that the U430 was selected. We have confirmed the superiority of this device by constructing headstages with many other FET types, including the U401 and U421 from Siliconix, NDF9406 (National Semiconductor), and 2SK146 and 2SK240 from Toshiba. None of these have exhibited noise levels as low as selected U430s.

At frequencies below about 100 Hz to 1 kHz, JFET input voltage noise is dominated by excess 'flicker' or $1/f$ noise, such that input voltage noise is better described by $e_n^2 \approx (4kT\nu/g_{fs})(1 + f_L/f^{\alpha})$, where α is near 1 and f_L is the '$1/f$ corner frequency', and varies from about 10–20 Hz (e.g., for the 2SK146) to several kHz. For the U430 f_L is subject to considerable production spread, but generally falls in the range of 100–1000 Hz. Since e_n is most important to noise in the measured current at high frequencies, moderate amounts of $1/f$ noise are relatively unimportant. In some FETs, however, it can be important for current measurements up to bandwidths of several kHz.

For a selected U430 and a 50 GΩ feedback resistor, the above considerations indicate that a headstage amplifier with a total current noise spectral density of as little as roughly $5 \times 10^{-31} + 2 \times 10^{-38} f^2$ (Amp^2/Hz) should be possible. This would result in spectral density of 10^{-31} Amp^2/Hz at 5 kHz for the headstage alone. To date, however, the best we have achieved is about 2.5×10^{-31} Amp^2/Hz at 5 kHz, or somewhat more than twice the predicted value. Part of this discrepancy may be attributable to excess high frequency noise from the feedback resistor; we presently use a 50 GΩ chip resistor from National Micronetics (kindly provided by F. Sigworth) which, as already noted, exhibits less excess noise than any other resistor we have tried, but may still be imperfect in this regard. The remaining extra noise is (somewhat arbitrarily) accounted for by the term $S_c(f)$ in equation (5). We have suspected for some time that the packaging of the FET may be responsible for some excess noise at high frequencies, since the material in which the chip and/or its leads is embedded must be expected to posses lossy dielectric properties and thereby introduce frequency-dependent leakage pathways. Sigworth (1983) has recently studied the effect of FET packaging on noise in the patch voltage clamp in some detail. He concludes that the extra noise arises from dielectric relaxation in the glass used to seal the wire leads into metal transistor cases and has shown that it is worse for transistors packaged in the small TO-71 package with small lead spacing (e.g., U401, NDF9406) than for those supplied in the larger TO-78 or TO-99 packages (e.g., the U430, U421, or the NDF9401, which is no longer available). Even so, in the case of the U430 it is our guess that noise generated by this mechanism may account for about one half of the observed power spectral density of the current noise from the headstage amplifier at frequencies in the 3–10 kHz range. Obviously, one solution to this problem would be to use unencapsulated FET chips; however, without the proper equipment it is very difficult to bond leads to such small (≈1 mm^2) devices.

2. *Seal noise*

If the membrane-glass seal were simply resistive then the spectral density, S_{sh}, of the thermal current noise associated with it would be given by $4kT/R_{sh}$, where k is Boltzman's constant, T is temperature (K) and R_{sh} is the resistance of the seal. For example, a seal resistance of 50 GΩ would produce $S_{sh} = 3.2 \times 10^{-31}$ Amp^2/Hz, and would be independent of frequency. The rms noise from such a seal would be only ≈0.06 pA for a bandwidth of current measurement of 10 kHz.

Unfortunately, it is unlikely that the membrane-glass seal is purely resistive in nature, due to the capacitance of the glass and particularly of the membrane which form the wall of the seal. The expression for the spectral density of the noise current arising from the seal in the presence of zero applied field is then:

$$S_{sh} = 4kT\, Re\ \ Y_{sh}\ , \tag{6}$$

where $Re\ \{Y_{sh}\}$ denotes the real part of the seal admittance, Y_{sh}. Since the precise nature of the membrane glass interaction is not presently understood, the exact form of Y_{sh} can not be predicted with certainty. It seems certain, however, that it will increase with increasing frequency from a low frequency value that is approximated by $4kT/R_{sh}$.

Empirical estimates of $Re\{Y_{sh}\}$ by Sachs and Neher (1983) (see also Sigworth, 1983) indicate that it may reach 2–3 $\times$ 10^{-10} Ω^{-1} by 5 kHz and increases approximately linearly with increasing frequency over the range 1–5 kHz. Our own measurements are in reasonable agreement with these, although a great deal of variability is found. In general, however, even for seals with a DC resistance in excess of 100 GΩ, S_{sh} will probably be about 2–4 $\times$ 10^{-30} Amp^2/Hz by 5 kHz and may be twice this large by 10 kHz. These values are roughly comparable to the noise arising from a low-noise patch clamp headstage by itself, and are also approximately equal to the noise contribution from pipettes fabricated with low-loss glass (e.g., Corning #1723 aluminosilicate, see below). However, while it may be anticipated that pipette noise and electronic noise associated with patch voltage clamping will be improved during the next few years, there is less reason to hope for any significant reductions in the noise arising from the seal. Thus seal noise may be the ultimate limitation of the resolution that is achievable with the patch voltage clamp technique. Our best estimates at this time suggest that a minimum of about 0.10 pA rms of noise will result from the seal at a bandwidth of current measurement of 10 kHz.

Equation (6) is only expected to strictly hold when there is zero applied field across the seal; i.e., under equilibrium conditions for the seal. When a voltage is applied to the pipette, the noise arising from the seal would exceed the Nyquist prediction (i.e., eq. 6). Excess noise associated with the seal has not as yet been subjected to systematic investigation.

3. *Pipette noise*

The pipette adds noise to the measured patch current by several mechanisms in addition to 'seal noise' discussed above. In the first place, the holder for the pipette is one source of stray capacitance, C_s, at the summing junction of the patch clamp headstage. Depending on its construction and the presence or absence of shielding, the holder can add roughly from 1 to 5 pF to C_s. This noise is described by equation (4) above, and is determined by the value of the input voltage noise of the headstage amplifier (2–3 nV/Hz$^{1/2}$ for a low-noise design). Similarly, the pipette itself adds to C_s. For an uncoated pipette this will amount to roughly 1–2 pF per mm of immersion in the bath. However, a thick coating of Sylgard extending several mm from some 50 to 100 μm from the pipette tip can substantially reduce this component of C_s, and render the noise relatively insensitive to the depth of immersion in the bath. The pipette and its holder can also be a major source of electrostatic pickup. Although this can be reduced with a shielded holder, such shielding will inevitably add several pF to C_s. We have found it to be sufficient to use a completely unshielded Teflon holder and simply ground all metal in the immediate vicinity of the pipette; adequate grounding of the microscope is imperative in this situation.

If the noise just described was the only contribution from the pipette to overall noise in the measured current, it would be relatively simple to reduce the contribution of the pipette to perhaps 1/3 or less of the noise of the headstage amplifier by itself, simply because C_s can readily be made small with respect to the 10–20 pF of input capacitance of the FET input stage. Under these circumstances the noise of the pipette would not be a limiting factor in achievable resolution with the patch clamp technique. Unfortu-

nately, the pipette contributes far more noise to the measured current than can be accounted for by its capacitance in conjunction with e_n. The most important additional sources of noise in most patch clamp situations are: (1) dielectric noise of the glass; and (2) noise arising from the creep of a thin fluid layer from the bath up the outer surface of the pipette wall. The latter source of noise can usually be completely eliminated by adequate Sylgard coating of the pipette as described below. However, the former source of noise is unavoidable and can only be minimized by selecting glasses for pipette fabrication that have the most desirable electrical characteristics.

No commercially available glass is adequately described by a bulk resistivity in parallel with a pure (lossless) capacitance. Instead, the wall of the pipette is better considered to be a pure capacitance in parallel with a bulk resistance and a lossy dielectric. An ideal capacitor has no intrinsic noise of its own (the real part of its admittance is zero), however, a lossy dielectric will generate noise (the real part of its admittance is non-zero). An approximate equivalent circuit of the glass wall of the pipette consists of a bulk resistance, R_B, in parallel with a pure capacitance, C_W, and a series RC (denoted by R_L and C_L). If the bulk conductivity is considered to be sufficiently small to be neglected, then the real part of the admittance, $Re\{Y_p\}$ of this approximation is $\omega^2 R_L C_L^2/(1 + \omega^2 R_L^2 C_L^2)$, and will exhibit thermal noise given by $4kT\ Re\{Y_p\}$ (Amp^2/Hz). The series RC leg of this circuit represents the dielectric relaxation of the glass. If it were to amount to 2 GΩ in series with 0.02 pF, then $Re\{Y_p\}$ forms an inverted Lorenztian with a corner frequency, $f_{1/2}$ of about 4 kHz and a high frequency limit of 5×10^{-10} mho. The admittance of any particular glass is surely more complicated than that of this simple model, but the behavior is qualitatively similar to what must be expected. A layer of Sylgard #184 places a second lossy dielectric in series with the glass (dielectric constant = 2.9, loss factor = 0.58%, as compared with 6.3 and 1.0% for aluminosilicate #1723) in series with the glass wall of the pipette and therefore can substantially reduce pipette noise.

Another source of noise that can be associated with the pipette arises from the creep of a thin film of fluid from the bath up the outer surface of the pipette as discussed by Hamill et al. (1983). They note that the distributed resistance of this film can be on the order of 100 MΩ and that it is in series with the capacitance of the pipette (also distributed) which is on the order of 3 pF. These figures provide estimates of the noise contribution from this mechanism that are generally in agreement with our own measurements. At high frequencies (3–10 kHz) this can result in an additional background noise in the measured current with a spectral density of the order of 10^{-28} Amp^2/Hz, which is greater than that of any other noise mechanism we have described or encountered. Thus reduction of this noise source is imperative to high resolution patch voltage clamping. Coating the pipette with any hydrophobic substance will substantially reduce this noise, but we prefer to use Sylgard, as recommended by Hamill et al. (1981) because it provides the greatest reduction of overall noise associated with the pipette of any substance that we have tried.

An additional source of noise that has seldom been discussed in regard to the patch voltage clamp (but see Levis, 1981) arises from the thermal voltage noise of the pipette in series with the capacitance of the patch membrane. This noise should have a spectral density, S_p, given by:

$$S_p = 4\pi^2 e_p^2 C_p^2 f^2, \tag{7}$$

where e_p is the voltage noise of the patch pipette ($e_p^2 \approx 4kTR_p$, where R_p is the resistance of the pipette), and C_p is the patch capacitance. The value of R_p typically ranges from about 2 MΩ to more than 10 MΩ, such that e_p will fall in the range of 180–400 nV/Hz$^{1/2}$ (i.e., as much as 200 times larger than e_n). The value of C_p can be estimated to typically be in the range of 0.01–0.1 pF (Sigworth and Neher, 1980), depending on the tip diameter of the pipette and the size of the 'horseshoe' of membrane that enters the tip. When extremely large amounts of membrane are aspirated into the tip it is not unreasonable to expect values of C_p as large as 0.2 pF. It is instructive to compare this noise to that arising from the input voltage noise, e_n, of the headstage; i.e., $4\pi^2 e_n^2 (C_{gs}+C_s)^2 f^2$. For a low-noise headstage, it is reasonable to expect $e_n = 3$ nV/Hz$^{1/2}$ and $C_{gs}+C_s = 15$ pF; with these parameters it will be found that a 10 MΩ pipette will contribute by the mechanism considered here as much high frequency noise as the headstage itself for $C_p = 0.11$ pF. Thus this noise source can be quite significant under unfavorable circumstances. It should also be pointed out that its existence makes it difficult to unambiguously assign a value to seal-generated noise.

The thermal voltage noise of the pipette will also generate noise in conjunction with the capacitance of the pipette wall. Hamill et al. (1981) report that this noise source amounts to roughly 2–5 MΩ in series with a tip capacitance of about 0.3 pF, and state that it contributes noise comparable to that of a 1GΩ resistor at 10 kHz. We believe, however, that this considerably overestimates this source of noise, since most of the resistance of the pipette resides within a few tens of microns of its tip, while the capacitance associated with this region is considerably less than 0.3 pF. We expect that this source of noise will generally be less than that arising from the capacitance of the patch itself.

4. *Noise in whole-cell voltage clamps*

The whole-cell variation of the patch voltage clamp technique is described in detail below (see under section Configurations). Briefly this technique involves the formation of a gigohm seal on the surface of a small cell followed by disruption of the membrane occluded by the pipette. If this disruption is successful, the gigohm seal remains, but the patch pipette interior is in direct communication with the cell interior. The approach thus represents a variant of the suction or 'suction-dialysis' voltage clamps introduced in the 1970s (e.g., Lee et al., 1978). In this situation all of the noise sources discussed above are still present (with the obvious exception of 'e_p–C_p' noise just discussed). However, the value of the headstage feedback resistor must be reduced into the range of 100 MΩ–1 GΩ to allow recording of the much larger currents without saturation. This increases the low frequency noise floor, and the thermal and shot noise processes of the cell membrane will also increase low frequency noise. At frequencies above a few hundred Hz, however, by far the dominant source of noise will be the cell capacitance, C_m, in series with the voltage noise of the pipette, e_p. This noise has a spectral density that is described by $4\pi^2 C_m^2 e_p^2 f^2$. For $C_m = 10$ pF and $R_p = 5$ MΩ (so that the thermal noise of the pipette is about 280 nV/H$^{1/2}$), this amounts to $3.2 \times 10^{-34} f^2$ Amp^2/Hz, or 8×10^{-27} Amp^2/Hz at $f = 5$ kHz (about 3000 times larger

than the noise of the headstage alone as shown in Fig. 5 at this frequency). Minimization of this noise requires that the pipette resistance be reduced to the smallest possible value. In some situations it may be desirable to return to the use of large tipped suction pipettes (e.g., Lee et al., 1978; see also Levis, 1981) with resistances in the range of 50–500 kΩ even if the gigohm seal is replaced by a seal of only ≈100 MΩ, and in this situation a floating Pt or Pt-Ag-AgCl shunt wire may be useful for reducing noise (Levis, 1981). It should also be noted that an excess $1/f$ noise component of e_p can safely be ignored in the case of the patch clamp because the magnitude of the current passed through the pipette is in the low pA range, but that excess noise of this type can be expected to become progressively important as the currents passed through the pipette increase (DeFelice and Firth, 1971) to nAmps, as expected in some whole-cell situations.

Summary of noise sources

The combined spectral density of all of the noise sources in the measured current, S_{nT}, is simply the algebraic sum of all noise spectral densities described above (i.e., S_f, S_{sh}, S_n, etc.). The variance, σ^2, of the background noise when observed after subsequent filtering is simply $\int_0^\infty S_{nT}|H(f)|^2 df$, where $|H(f)|$ is the transfer function of the filter used. The square root of the variance is the rms value (about 1/5 of peak-to-peak) of the background noise.

At the present time the noise of the headstage amplifier is not the limiting factor in the resolution achieved in our patch clamp measurements. Under favorable circumstances the noise of the headstage alone (see eq. 5) is roughly equal to that which we estimate arises from the seal, and is somewhat less than that arising from the pipette. Noise spectral density from a recent headstage design by itself (curve a) and from this headstage with Sylgard-coated pipettes fabricated from three different kinds of glasses sealed to Sylgard (curves b–d) are illustrated in Fig. 5. Although membrane to glass seals usually produce somewhat more noise, we have with each glass type achieved seals to our cells with noise (for small applied fields) that closely approach those shown in this figure.

PATCH CLAMP METHODS

Glass technology

The formation of the gigohm seal requires an interaction between the glass of the electrode and the cell membrane. The nature of this interaction is not presently understood but it seems probable that some form of chemical bond occurs between membrane and glass. A simple model of interaction which places the seal resistance in a fluid filled cylindrical ring between the membrane and the inner wall of the electrode predicts that resistances in the tens of gigohms can occur only if the membrane and the glass are separated by distances of a few angstroms. These are distances anticipated if the forces result from molecular interactions.

Specialty glasses

Since this interaction between membrane and glass is imperative for high resolution patch clamping, careful attention to the glasses being used seems warranted. We have spent considerable effort investigating commercially available glasses for their suitability for use in patch clamping. Since we do not propose to understand how the membrane and glass interact in molecular terms, our investigation of these glasses has been largely empirical. We have simply selected glasses whose specifications seemed promising, obtained the glasses from speciality suppliers, and used the glasses to fabricate electrodes for subsequent patching of lens epithelial cells.

There are three general sets of properties of glasses which should be important for patch clamp electrodes. These are thermal, electrical, and sealing properties.

Thermal properties

The thermal properties of patch electrode glass are important from two standpoints. First, it is desirable to have a glass which pulls at a sufficiently low temperature that many pipettes can be fabricated using the same heater coil without significant change in the geometry of the coil. Such geometry changes occur more quickly as the temperature of the coil increases. Pulling glasses which soften at high temperature, such as aluminosilicate glasses, results in progressive sagging of the heater coil which not only requires frequent changing of coils but also causes the coil to change its heating properties from day to day as the spatial relationship of the glass and coil changes with time. Thus, it is easier to pull electrodes with consistent geometry when glasses which soften at lower temperature are used. Second, it is also desirable to have a glass where the changes in the tip caused by heating are easily visible through the microscope. Some glasses, like soda lime glasses produce an optically indistinct endpoint to fire polishing whereas glasses like Corning 7052 produce easily discernible optical changes with heating and allow fire polishing to an optically precise endpoint. In general, optically precise endpoints occur in glasses which soften at higher temperatures. Many commercially available glasses provide a suitable compromise between these two thermal requirements.

Electrical properties

There is no a priori way to know which electrical specifications of the glass are important for patch clamping. We believe that glasses with the lowest loss factors, highest volume resistivities, and lowest dielectric constants should result in the lowest current noise but the relative importance of each of these factors is not yet clear. Table 1 shows glasses which look promising on the basis of these specifications. We have obtained most of these and have evaluated their use for patch clamping. Each glass was tested by fabricating a patch electrode from it, coating the electrode to within 50–100 microns of the tip with Sylgard #184 (Dow Corning, Midland, MI), sealing its tip to Sylgard in the bottom of a saline filled chamber, and measuring the power spectrum of the current noise of the sealed electrode. The results of these tests suggest as would be expected, that glasses with a low loss factor often have low noise. However, high lead glasses have low loss factors but other than # 8161 do not have low noise and thus other properties must be involved. Resolving these issues is further

TABLE 1

Specifications for various commercially available glasses

Glass	Loss factor %	Log 10 vol resistivity at 250°C	Dielectric constant	Softening temp. °C	Description
7070	0.25	11.2	4.1	–	Low loss
8161	0.50	12.0	8.3	604	Potash lead
7760	0.79	9.4	4.5	780	Borosilicate
EG-6	0.80	9.6	7.0	625	Pot. soda lead
0120	0.80	10.1	6.7	630	Pot. soda lead
EG-16	0.90	11.3	9.6	580	High lead
7040	1.00	9.6	4.8	700	Kovar seal
KG-12	1.00	9.9	6.7	632	Pot. soda lead
1723	1.00	13.5	6.3	910	Aluminosilicate
0010	1.07	8.9	6.7	625	Pot. soda lead
7052	1.30	9.2	4.9	710	Kovar seal
EN-1	1.30	9.0	5.1	716	Kovar seal
7720	1.30	8.8	4.7	755	Tungsten seal
7056	1.50	10.2	5.7	720	Kovar seal
3320	1.50	8.6	4.9	780	Tungsten seal
7050	1.60	8.8	4.9	705	Series seal
7740	2.60	8.1	5.1	820	Pyrex
1720	2.70	11.4	7.2	915	Aluminosilicate
R-6	5.10	6.6	7.3	700	Soda lime
0080	6.50	6.4	7.2	695	Soda lime
Sylgard	0.58	13.0	2.9	–	#184

Loss factor = loss angle × dielectric constant × 100

complicated by the fact that a coating of Sylgard reduces the spectral density of high frequency noise attributed to pipettes fabricated from any particular glass by nearly an order of magnitude. Clearly, glass noise is an important area for future investigation.

Sealing properties

At present, there is no known way to predict which glasses are most likely to seal to membranes. Membranes differ significantly in their composition and function from one cell to another and even from one part of the cell to another. They also differ in their extracellular surface coatings. Thus, there is no reason to expect the existence of some 'super glass' which will be optimal for all cells. In our opinion, the only way to test a glass for sealing suitability with a particular cell is to make patch electrodes from the glass and try to form seals with the cells. The glass used in most of the experimental work described here, Corning (Corning, NY) #7052 Kovar sealing glass, was selected because of its electrical specifications. We were pleasantly surprised that we obtained 400 seals in our first 406 attempts with lens epithelial cells. This glass is quite unusual in that it is possible to obtain multiple gigohm seals with the same electrode, as many as 7 in our experience.

Since these early tests, we have acquired almost all of the glasses listed in Table 1 and have tested them for their ability to seal to lens epithelial cells. We have yet to find a glass where a glass-membrane seal is impossible. However, for our cells, the probability of obtaining a seal varies greatly from glass to glass. Glasses in the Corning 7700 series such as 7740 (Pyrex) or 7720 will occasionally seal to our cells but seals are infrequent and not very stable. Glasses in the Corning 7000 series seal much better to our cells with #7052 and #7056 being particularly outstanding in this regard. However, seals with #7040, #7050, and #7070 occur with sufficient frequency and quality that these glasses should also be useful for patch clamping. Soda lime glasses such as Corning #0080 or Kimble (Toledo, OH) #R-6 readily produce stable seals but have higher noise properties than the harder glasses. To date, we have found no glass with noise properties as low as Corning #1723 (Aluminosilicate). This glass also seals well to our cells and the stability of the seals is considerably better than 7700 series glasses but worse then either the 7000 series glasses or soda lime glasses.

Obtaining specialty glasses

Specialty glasses may be obtained from firms such as Wilmad Glass (Buena, NJ) or Garner Glass (Claremont, CA) where within reasonable limits it can be redrawn into tubing of appropriate size for patch electrodes (we presently use 1.65 mm O.D., 1.2 mm I.D. but believe that thicker walls will yield less noise). These firms can pull the same glass to different O.D.s, I.D.s and wall thicknesses to support the investigation of the effect of glass geometry on its noise properties and ability to seal to membranes.

Pulling electrodes

The electrodes are pulled on a David Kopf vertical puller which is modified to drive the heater coil at constant power. Although we are able to pull very consistent electrodes from day to day using this constant power circuit, constant power is not really necessary for acceptable results. Maintaining the heater at approximately constant current by adjusting the rheostat on the Kopf Puller to keep the metered current constant is sufficient, although somewhat less convenient, for producing repeatable pipettes. An air shield should be placed around the heater coil since air currents dissipate the heat from the coil and produce differences in heating from minute to minute. We pull electrodes in almost the same way described by Hamill et al. (1981). According to their protocol, the glass is first pulled to an hour glass shape by mechanically stopping the pull before the glass separates into two pieces. The narrowed region of glass is then repositioned into the heater coil and pulled a second time until separation occurs. Although our electrodes are routinely pulled in two stages, the use of more stages provides even more flexibility in final tip shapes. The very blunt tip tapers recommended by Hamill et al. (1981) are not the best for sealing our cells. The main virtue of the blunt tip taper is the minimized tip access resistance. This resistance is important for voltage clamping an entire cell through the patch electrode but is less important for measuring from isolated patches of membrane. For sealing our thin epithelial cells optimally, we fabricate pipettes that have longer tip tapers and a few microns of nearly parallel wall just behind the highly fire polished tip. Experimenting with different tip geometries is very useful when trying to determine the best way to form seals with any particular cell type.

Pulled electrodes may be stored for some time before use. They should be stored so that no foreign substances get on their surfaces. For example, we initially stored our electrodes in a container with the electrodes held in Plasticine. These electrodes were useful in producing seals for about 10 h after pulling and then their surfaces became greasy. We subsequently used dry, sealed jars with the electrodes held in notches in a rubber ring. These electrodes have produced seals weeks after pulling.

Electrode coating

There is a substantial noise component that comes from a fluid layer that creeps up the electrode tip once it is immersed in the bath. This problem can be minimized by painting the electrode with a hydrophobic substance which prevents the creep of fluids. We have tested a large number of such substances and have found nothing more effective in reducing electrode noise than the #184 Sylgard previously recommended by Hamill et al. (1981). Sylgard #182 is considerably less effective. Sylgard #184 is very convenient since it can be stored in a freezer for about two weeks after it is mixed. After about 4 h at room temperature, the viscosity of the Sylgard becomes optimal for applying a very heavy coat but it can be used immediately out of the freezer. We paint the electrode tip using another electrode which has been dipped into the Sylgard. The painting is done under a dark field dissecting microscope which gives outstanding visibility of the walls of the electrode and the meniscus of the Sylgard. Many laboratories including ours have noted that Sylgard sometimes creeps toward the electrode tip during coating and may coat or fill the tip. Even if the Sylgard is burned away during a subsequent fire polishing operation, the probability of obtaining seals with such electrodes is greatly reduced. We avoid this problem by holding the electrode with the tip up at an angle to the ground during coating to maintain a constant gravitational force away from the tip. We then paint a very thin ring of Sylgard as close to the tip as desired. The ring must go entirely around the electrode. The electrode is then clamped in the bottom clamp of the Kopf puller (tip up) and moved up into the coil which is heated to a temperature just below that which causes the coil to glow. After about 15 s of curing, the electrode is returned to the dissecting microscope where it is painted with as heavy a Sylgard coat as desired, the previous Sylgard ring apparently keeping the new Sylgard from creeping forward. The final curing is done with a heat gun with the tip of the electrode pointing up. This procedure avoids movement of Sylgard into the tip and we have achieved higher seal rates than before adopting the approach. The Sylgard does at least two things to improve electrode noise. One is to prevent the fluid creep mentioned above. The second is to improve the noise properties of the electrode by placing a second insulator in series with the wall of the electrode thus reducing its capacitance and its bulk conductance. For this second action, it is desirable to paint as close to the tip as possible but in so doing the probability of painting over the tip goes up considerably. We find that we can consistently paint to within 50–100 microns of the tip with no difficulty. In our opinion, except in those situations where extremely low noise is of utmost importance, painting to this distance from the tip is sufficient. It is important that the bathing fluid not be allowed to rise above the level where the Sylgard terminates. When the fluid touches the bare glass, the noise is essentially the same as if the electrode were not

coated. Coating near the tip is more important for noisy glasses like soda lime, than for borosilicate or aluminosilicate glasses whose inherent electrical properties are better. It is desirable to coat soda lime glass as close to the tip as possible but to us it seems far better to find one of the available hard glasses that will work with the preparation under investigation.

Fire polishing

The electrode tip is fire polished by bringing it close to a piece of thin platinum wire which has been coated with the same glass used for constructing the electrodes. In our apparatus, the platinum wire is connected to the output of a 6-V filament transformer which in turn is connected to the output of a variable transformer. The variable transformer gives a sufficiently sensitive adjustment of the current through and thus the heating of the platinum. The platinum wire is bent into a hairpin and is mounted on a micromanipulator which allows it to be positioned in the field of the microscope used for the fire polishing. The electrode is placed in a groove of an acrylic plastic slide of the same size as a standard microscope slide. This slide is moved by the mechanical stage of the microscope to bring the electrode tip close to the hairpin of the platinum wire. During the polishing operation, we continually move the electrode back and forth along a line parallel to the tangent of the platinum hairpin. This action ensures symmetrically rounded tips.

In our experience, the ability to obtain seals on lens epithelial cells is quite independent of the amount of fire polishing. Electrodes pulled to about the desired size and then rounded slightly by polishing, seal easily to our cells. However, such electrodes also easily penetrate the cells and thus require more care in placing the electrode on the cell and in applying suction. For cells that are only 2–5 microns in thickness, it seems better to pull tips which are larger in tip diameter than desirable for final use. These can be fire polished until the tip opening is the desired size. With the hard glasses we use, considerable control can be exerted over the final geometry of the tip depending on how it is fire polished. If the tip is placed to within a few microns of the platinum wire and the current is reduced to lower the wire temperature, the fire polished tip narrows, has nearly parallel walls near the opening, but is very rounded at the tip extremity. If the tip is placed a few hundred microns from the platinum wire and the wire is maintained at a considerably higher temperature, the tip does not narrow but simply rounds and assumes an extremely blunt appearance, similar to that recommended by Hamill et al. (1981). For long electrode tips, the fire polishing may be required both before and after Sylgard coating. Sylgard changes the thermal properties of the electrode near the tip and does not allow the heat to be dissipated as easily. Thus, when the tip is fairly long, it may sag as it is heated and produce a bend which begins at the forward termination of the Sylgard coating. This may be useful if a bent tip is required to approach a cell at 90 degrees to its surface tangent but in general, a bent tip is a nuisance. The bend is avoided if the tip is fire polished both before and after Sylgarding. A light polishing after coating removes surface molecules of Sylgard which may have covered the rim of the electrode.

Electrode filling

Usable electrodes can be filled by a combination of suction and back filling. A 10-ml syringe fitted with a small rubber holder like that used for filling Drummond Microcaps (Broomall, PA) works well. A strong suction is applied for 5–30 s depending on the size of the tip. This fills the tip. The remainder of the electrode is back filled using a syringe fitted with a 0.22 micron Swinnex filter (Millipore Corp., Bedford, MA) and with either a 24–26 guage needle or a piece of polyethylene tubing cemented to the syringe. It has been reported that the solution inside a stainless steel syringe needle changes its pH and decreases the probability of obtaining seals (Corey and Stevens, 1984). Thus, one should be certain that the contents of the needle are flushed before backfilling the electrode. These filling procedures usually leave bubbles in the shank of the electrode, which can be removed by tapping the electrode. The difficulty in removing the bubbles increases as the tip size decreases. In our experience it is always possible to remove bubbles even if the electrode tip is fire polished to complete closure. Removal of bubbles is necessary for three reasons: (1) the existence of a bubble reduces one's ability to control the suction on the membrane; (2) the bubble increases the electrode resistance; (3) we have noted that seals obtained with a bubble in the electrode have excess noise. After filling the tip of the electrode to the desired level, the back of the electrode is dried with a fine stream of clean gas. In addition, gas is blown through the suction line in the electrode holder to dry fluid there since fluid in the electrode holder is a noise source.

Obtaining seals

Electrode holder and input connector

Gigohm seals in general result after pressing a patch electrode against the cell membrane and then applying suction to the back of the pipette. Although the suction is not always necessary, it is the important advance which has produced a high incidence of gigohm seals (Neher, 1981). Therefore, careful attention should be paid to the quality of the suction apparatus. There are now a wide variety of suction electrode holders available for patch clamping (Medical Systems, Great Neck, NY, WP Instruments, New Haven, CT, E.W. Wright, Guilford, CT). We use a teflon holder of our own design but it offers few significant advantages over those commercially available. Most commercially available holders are designed to be used with a BNC connector on the patch clamp headstage. Our initial experience with such connectors was bad since some produced a leakage path between the input and ground. Standard isolated BNC connectors which do not use teflon isolation are particularly bad. The insulating material of the BNC produced considerable excess leakage and dielectric noise which was frequency-dependent. We designed a teflon input connector which eliminated this problem. A simple test for the adequacy of the connector is to unsolder the headstage input connector from the FET and feedback resistor. The background noise of the headstage should not be significantly increased by the connector. It should be noted that the input lead to the FET should not make contact with the printed circuit board since the leakage through the board will significantly increase the noise of the headstage. The electrode holder must provide a flat surface for the electrode to seat against

otherwise when suction is applied, the electrode moves away from the preparation and seals rarely occur. It must also have no air leaks. Our major reason for periods of low seal probability has been tiny electrode holder leaks. In each of these periods, it became clear that considerable suction could be produced but that the suction was dissipated over many seconds of application. Replacement of the electrode gaskets always solved this problem. Another problem associated with sealing came from the application of a positive pressure to the electrode when it went from air into the bath, a procedure recommended by Hamill et al. (1981). Although this procedure seems very reasonable, it proved bothersome for us because the eddy currents produced by flow from the tip delivered particulate matter from the bath directly to the tip. The problem went away when we stopped using positive pressure. We also found that it was important to make contact with the cell membrane within 2–3 min after placing the patch electrode in the bath. Beyond this time period, seals rarely formed.

Suction methods

The electrode suction has been produced by three methods. One is to simply suck by mouth on the line going to the electrode holder. Although this method works very well and is widely used, we do not use it since it does not allow quantitation of the degree of suction. The second is to use a threaded syringe like those from AM Systems (Everett, WA). A threaded syringe allows precise control of the suction but does not allow the quick changes in suction possible with mouth suction. The third technique which we prefer uses a 10-ml syringe with a suction line which can be disconnected rapidly. Any degree of initial suction can be obtained by adjusting the starting volume of the syringe and then replacing the suction line. For example, with the syringe initially at 5 ml, the maximum suction that can be produced is about (–)1 atmosphere. The rate of change of the suction is also far less than if the syringe plunger had been placed initially at say 0.5 ml. An initial placement of the syringe plunger at 9 ml allows only a small suction with a small rate of change. With a little practice, this versatile suction system works well.

Observing seal formation

In obtaining gigohm seals, one commands a small voltage to the voltage clamp while the electrode is in the bath. If a square pulse command signal is used, a square pulse of current sufficient to clamp to the command voltage results. This current pulse is observed on the oscilloscope while sealing is being attempted. It is useful to make the initial contact of cell and pipette under direct observation. This requires good optics. Techniques such as interference contrast or Hoffman modulation contrast which take an optical slice and thus have limited depth of field are particularly useful for assessing close proximity of the electrode tip and cell surface. In our experience, the highest probability of seal success comes when the final movement of the electrode occurs in a direction parallel to its long axis. When the electrode touches the surface of the cell, the resistance should increase and result in a smaller current pulse to achieve the commanded voltage. If this does not occur, for example if there is simply a transient jump in the current trace without a resistance increase, the probability of obtaining seals with our cells is small. The application of suction should cause the resistance to

increase until the gigohm seal occurs. For our cell, if no resistance increase occurs when the electrode is pressed against the membrane, little resistance increase will occur with suction and a gigohm seal is unlikely. We observe the seal process at 5–10 kHz bandwidth so that the progression of the seal formation can be observed from the reduction in wideband noise. For lens epithelium from 6 different species of animals, the initial degree of indention of the cells is important for obtaining a high probability of gigohm seals, different species requiring different indentations. This is a parameter to be determined for each new preparation. The maximum suction and the rate of change of suction are also important and again must be investigated with each preparation. For our cells, we find it useful to start with the syringe at about 7.5 ml, to slowly increase its volume to about 9.5 ml and to wait until the seal resistance stabilizes. Often the gigohm seal occurs during this operation. If not, removal of the suction line, repositioning of the syringe to 0.5 ml, replacing the suction line, and increasing the syringe volume to 0.7–0.8 ml will often result in gigohm seals. Under ideal circumstances, the gigohm seals form quickly (within 5 s). In our experience, such seals are the most stable. However, some stable seals have occurred even after 5 min of suction.

We have noted one problem that can occur when a seal forms which is of sufficient concern that it merits discussion. The patch electrode and the bath electrode often have an offset voltage between them which must be zeroed with both electrodes in the bath. When the gigohm seal forms, this offset can change by as much as 60 mV. The source of this new offset is presently unknown. Sometimes it rapidly decays to zero but sometimes it remains elevated for the duration of the experiment and provides a driving voltage across the channels when none is desired. This 'spurious' offset must be rezeroed before proceeding with experiments; otherwise, the reversal potentials determined from the experiments will be in error by the amount of the offset. The problem is worst for on-cell patches but does not occur in all preparations. For example, it always occurs in *Rana pipiens* lens epithelium but never occurs in mouse lens epithelium. Often the offset goes away when the patch is excised and thus a patch which had been adjusted for zero offset on the cell, may suddenly have a large offset at the time of excision.

With proper optics, it is often possible to see the omega shaped piece of membrane drawn into the pipette by suction. We have been surprised to see how large the membrane patch can be. On occasion it extends more than 20 microns up the tip and contains much more membrane surface than one might have guessed (see Sigworth and Neher, 1980).

Epithelial patch clamp set-up

The microscope

To date, most patch clamp investigations have been done on isolated cells or on cells in tissue culture. With these kinds of cells, it is convenient to use inverted microscopes since they have long working distance condensers which leave room for easy placement of a patch electrode between the condenser and bath at almost any angle desired. In addition, they support optical techniques such as Nomarski and Hoffman modula-

tion contrast. Objective working distance is no problem since it must only be long enough to exceed the thickness of a petri dish and one cell. In addition, since the viewing occurs from below the specimen, there is no problem with optical distortion due to the meniscus created by the pipette entering the fluid bath. Its main disadvantage is that the cell-electrode contact must be viewed through the cell from the bottom. Since single cells are usually quite transparent, this causes few difficulties in isolated cell preparations or tissue-cultured preparations. Unfortunately, many epithelia cannot be dissociated and have not been grown in tissue culture. Even if they could be, there would be considerable merit in recording from the naturally occurring preparation. Also, many epithelia contain multiple layers of cells and sometimes even have muscle and connective tissue layers attached which are not transparent. For these epithelia, an inverted microscope would not work.

We wanted to investigate our preparation without harsh dissociation or tissue culturing. Thus we had to develop an optical system to circumvent the difficulties inherent in the inverted microscopes in common use. This system has proven to be so useful that we will briefly describe it here. We use a microscope modified for us by Frank E. Fryer Co. (Carpentersville, IL). The microscope uses mostly standard Nikon parts and optics but is modified so as to fold back in the middle to allow movement of the erect image binocular head and objectives away from the preparation. This allows ease in placement of the preparation in the bath. The microscope is mounted on a micrometer driven x–y table so that the entire microscope can be moved with respect to the preparation to allow precise measurement of cell dimensions. This microscope and x–y table is similar to one used previously by Valdiosera et al. (1974). Standard compound microscope objectives which support interference contrast or Hoffman modulation contrast have only a few millimeters working distance and severely limit the penetration angle which can be achieved with patch electrodes. A new series of extra long working distance metallurgical objectives from Nikon have magnifications of 20× and 40× and working distances of about 10 mm while retaining a numerical aperture of 0.5 for the 40× objective. This working distance supports penetration angles of about 45 degrees which is sufficient for sealing cells as thin as 2 microns, about the minimum thickness of our epithelial preparations. These objectives are simple bright field objectives and as delivered are incapable of taking optical slices which are desirable for patch clamping. Therefore, we modified the microscope to implement the Schlieren principle (see Axelrod, 1981 for a description of the technique). This principle can be implemented with a piece of opaque tape on the condenser and a piece of opaque tape at the back of the objective and produces optical images very similar to Normarski or Hoffman contrast. Our cells are clearly visible by this technique and it is quite easy to place the electrode within 2 microns of the cell surface because of the limited depth of field which the technique produces. Initially the visibility was not good because of the distortion caused by viewing the specimen through the meniscus formed between the electrode and the bath. This problem was solved by placing a cut microscope slide over about 2/3 of the bath so that the preparation could be viewed through the slide. The microelectrode was lowered under the edge of the slide so that when its tip approached the cell surface, it was also being viewed through the microscope slide. This technique was suggested to us by Dr.

Richard Horn. In addition to providing excellent visibility, the slide also reduced rippling of the bath surface and thus reduced a vibrational noise component in the current measurement.

The micromanipulator

The proper choice of micromanipulators can be important to successful patch clamping. Most investigators have chosen to use a three-axis hydraulic micromanipulator for moving the electrode and headstage. This hydraulic micromanipulator is usually mounted on a fairly coarse micromanipulator for gross positioning. Such a system works well if the patch is to be torn away from the cell. However, the hydraulic micromanipulators tend to drift with time and thus it is difficult to measure from patches on the cell for extended periods. Frequently, the electrode either drifts forward and penetrates the cell or drifts backwards and tears the patch away from the cell. We have found that the MR and MV series of micromanipulators from Klinger Scientific (Richmond, NY) are exceptionally stable and capable of repeatable 1 micron movements in all directions. They allow placement of the electrode tip very close to the cell surface to be patched. The final positioning is done with a high accuracy one-dimensional DC motor driven slide (Klinger MT-50). This slide allows movements of 0.1 micron increments, does not drift, and introduces no additional noise in the patch clamp except when the motor is rotating. This system supports all configurations of the patch clamp adequately.

The chamber

The bath in which the preparation is mounted is also important. In our experience, the lens epithelial cells deteriorate quickly and become unsealable when they are bathed with solutions containing fluoride, EGTA, or highly elevated potassium chloride concentrations. Thus, we have found it unacceptable to superfuse the preparation bath with solutions very different from normal Ringer solution. Rather, we use a two bath chamber for studying excised patches. The front bath contains the cells and a standard Ringer solution with or without drugs. The back bath contains any desired bathing solution which can be changed without fear of destroying the cells located in the front bath. Each bath has its own ground and a switching arrangement which allows either bath to be connected to the ground of the headstage. Movement from one bath to another is accomplished by over filling both baths with the same solution so that a fluid bridge is formed between them. The pipette tip is moved in this fluid bridge to the desired chamber and fluid is then withdrawn to disrupt the bridge.

Preparation of lens cells

The single channels which we report here were recorded from adult lens epithelium of numerous animals including bull frog, grass frog, mouse, chicken, rat, and rabbit. In general, no enzymatic treatments are required to prepare the cell surfaces for sealing. The intact preparations are simply pinned with 000 stainless steel insect pins to an appropriately sized Sylgard disc. This disc is pinned into the front bath of our chamber to Sylgard which lines the bottom. This arrangement allows convenient

removal of the preparation and supports measurement from many different preparations during a single experiment.

On occasion, the cells have a surface coating which is a milky looking substance which partially obscures the cell boundaries making them visually indistinct. Frequently, cells with this coating can be sealed without further treatment. If the surface coating is particularly severe and will not allow seals, often treating the cells for 20–30 min with a solution containing 10 μg/ml of Trypsin in Ringer solution will improve their sealability. Collagenase has not been useful. The cells are very sensitive to osmotic swelling and shrinking and seals are more easily achieved in cells maintained in solutions of the proper tonicity. In our experience, with swollen cells, the patch electrode usually penetrates the cell when even a small amount of suction is applied. Our usual preparation of cells, bathed in an isotonic solution, is good for at least 4 h but rarely lasts longer than 8 h. Beyond this time, it becomes very difficult to obtain seals.

PATCH CLAMP CONFIGURATIONS

The patch clamp is a versatile technique which can be used in a number of configurations (Hamill et al., 1981, p. 93). Each of these configurations has its own strengths and weaknesses and in this section we will describe some of the most obvious.

On-cell patch

The on-cell patch is perhaps the most physiologically relevant. In this mode, the patch electrode is sealed to the membrane of an intact cell so that the outside of the membrane faces the solution in the pipette and the inside of the membrane faces the cytoplasm of the cell. Substances and structures inside the cell which control the operation of the channel proteins are presumably intact and free to exert their influence. In addition, the channels have the cell resting voltage across them when the lumen of the patch electrode is held at ground. The single channel currents can be increased by changing the pipette voltage to add to the driving force provided by the resting voltage. The channels remain essentially voltage-clamped because the currents which flow through single channels located in the patch are sufficiently small that when they flow through the input resistance of the rest of the cell (as they must since the rest of the cell is in series with the patch), the IR drop across the rest of the cell produces no appreciable change in the trans-patch voltage. For channels that do not reverse near the resting voltage, larger total fields can be produced without seal breakdown in this configuration than in any other we have tried.

One disadvantage of the on-cell patch is that the membrane potential is not known unless it is measured with a second voltage measuring microelectrode, a formidable task in small epithelial cells. Thus, in general, the current voltage relationships obtained are with reference to the resting potential of the cell and not with reference to an absolute potential. A second disadvantage is that it is difficult to change the solution on either side of the patch. Thus, channels in any one patch can be studied

easily with only one combination of solutions across them and the composition of the inside solution is largely unknown. Cull-Candy and coworkers (1982) have described a technique for changing the solution in the pipette but few workers have yet adopted it. Also, because of drift problems with most micromanipulators and movement caused by changing of solutions, on-cell patches are difficult to maintain for an extended period.

Inside-out patch

A second configuration is referred to as the inside-out patch (Horn and Patlak, 1980). This is obtained by initially forming an on-cell patch and then quickly withdrawing the electrode from the cell. When this operation is successful, the patch of membrane sealed to the electrode is torn away from the cell and remains bridged across the lumen of the pipette. The outer membrane surface of the patch faces the solution in the electrode whereas the membrane surface previously facing the interior of the cell is now exposed to the bath. If the bath is grounded, the voltage across the patch of membrane is (with reference to the inside of the cell), minus the voltage in the patch electrode. This is a particularly useful configuration for two reasons. One, the bathing solution can be repeatedly changed thus allowing records with a wide variety of chemical as well as electrical gradients across the channels. Two, since the patch of membrane is the same patch that existed when the pipette was sealed to the cell, the same channels seen in the on-cell patch should still be seen following the excision. This allows one to compare the behavior and selectivity of the channel both on and off the cell.

This inside-out patch has a few major disadvantages which can limit its usefulness. Often when the patch is torn away from the cell, a vesicle forms. This presumably forms when flaps of excess membrane adhering to the outside of the pipette rim come together to form an enclosed sphere of membrane with solution trapped inside of it. It is not possible to know the composition of the solution in the vesicle but it is possible for it to be sufficiently different from the bath that an unknown electrochemical driving force can exist across the channel. Moreover, channel currents must flow through the second membrane in series with the patch of membrane across which one desires to record. This second membrane is a series impedance and acts like an AC high pass filter and a DC voltage divider so that single channel currents are not of the correct amplitude and are not rectangular. Rather, they droop due to the filtering of the second membrane. Data from such a situation is obviously not very useful. There are a few methods that have been reported to break these vesicles. One is to place the tip of the electrode in a solution containing fluoride (Horn and Patlak, 1980). In our experience, this often does not break the vesicles. A second method is to lift the pipette into the air for a few seconds and then return it to the bath. For our cells, this often works but frequently causes the loss of the entire patch rather than the specific loss of the second membrane of the vesicle. This procedure works best when the seal resistance is high, for example in excess of 20 gigohms. For lower resistance seals, disruption almost invariably results. A third procedure is to change the bathing solution to one containing low Ca with EGTA. This procedure works best for our cells

but does not break all vesicles. Of course, these procedures can be combined. For example, the tip can be lifted into the air and then placed in a low Ca-EGTA solution.

Outside-out patch

A third configuration is known as the outside-out patch since in it the outer surface of the cell membrane faces the bath. This type of patch is achieved by first establishing a gigohm seal with the cell. The membrane patch is then disrupted either by additional suction or by pulsing the patch with a large voltage step. We have found that a 1 V step for 100 ms repeated as required works far better for our cells than additional suction since the suction technique usually results in loss of the seal rather than disruption of the membrane. Following disruption of the patch, the electrode is very slowly withdrawn from the cell. As this occurs, a tube of membrane which continues to be connected to the cell is formed. When this technique is successful, the membrane tube finally snaps loose from the cell and coalesces to produce a vesicle of membrane open to the pipette with the gigohm seal intact. The outer membrane surface faces the bath and the inner membrane surface faces the pipette lumen. This outside-out patch is particularly useful for at least two reasons: (1) double, sealed membrane vesicles do not form in this configuration since the membrane bridging the lumen of the pipette is removed before withdrawing the pipette, and the two membranes necessary for forming a sealed vesicle cannot exist; (2) substances which have their action on the outside of the cell can be tested more easily than with inside-out or on-cell patches where such substances have to be placed in the pipette. With our cells, there are almost always channels in the outside-out patches whereas in the inside-out patches, particularly from grass frogs, there are sometimes no channels present. The reason for this is not clear but may be as simple as there is an undetected vesicle in the inside-out patches where no channels are seen or that the outside-out patches have a larger area than inside-out patches. In our experience, the outside-out configuration has the disadvantages that the patch is generally noisier, the average seal resistances are lower, and the patches are more easily disrupted by solution changes than are the inside out patches.

All three of the patch configurations allow crude spatial localization of the channels. Since it is well known that different regions of epithelial cells have different ionic conductances, the patch clamp is likely to be useful in determining precisely where the channels are located.

Whole-cell clamp

The final configuration is the whole cell clamp. This is not really a patch clamp since in this situation the entire cell is voltage-clamped through the patch electrode. This whole-cell clamp is achieved by first forming a gigohm seal on the cell and then disrupting the patch with suction or voltage pulses as previously described. When this has been successfully accomplished, the inside of the cell and the inside of the patch electrode are in direct communication. The solution in the pipette and the cytoplasm equilibrate. The potential inside the cell is ideally equal to the potential inside the pipette which is controlled by the voltage clamp circuit. It is important that the access

resistance of the pipette be as small as possible since as current flows between the cell and the pipette, there is a voltage drop across the tip of the pipette in proportion to its access resistance. This causes the pipette and the cell interior to be at a different voltage and thus the cell will not be controlled at the desired command voltage. Properly constructed, blunt tapered electrodes along with series resistance compensation circuits will minimize the difference between the pipette potential and the cell potential. Electrodes which might be very useful for patch clamping may be of no use in whole cell clamping if their resistance is high and if there is a region near the tip where the walls of the pipette are parallel.

This whole-cell clamp has not yet been exploited in our measurements for reasons which will be common for most epithelia. Most epithelia occur in flat sheets with adjacent cells being electrically coupled. Therefore, the measured current arises from more than one cell and is not in general interpretable. Although it is possible to make the cells uncouple by using acidic or high Ca filling solutions, the close proximity of adjacent cells with restricted extracellular clefts will result in extracellular voltage drops which are spatially nonuniform even if the intracellular compartment is spatially uniform. Injection of H^+ or Ca^{2+} to produce uncoupling would have the added complication that these substances have known direct or indirect effects on many channels. Thus it is clear that the whole cell clamp works best on single, isolated cells. This requires the use of cultured epithelial cells early after plating when they still occur as isolated cells or dissociation of either tissue cultured preparations or naturally occurring epithelial preparations so that isolated single cells are available. The method of whole cell clamping will be very important in epithelial studies because it will allow quantitation of macroscopic conductances in cells too small to be voltage clamped by conventional means.

A potentially valuable use of the whole-cell clamp is in the measurement of membrane ion pump noise. If most of the channel conductances can be blocked by some means, measurement of the power spectrum of the current noise of the cell can in principle allow one to measure the kinetics of ion pumps. This promising use of the whole cell clamp is described in the following simple analysis.

Treatment of the *Rana pipiens* lens with 1×10^{-4} M ouabain causes about a 10 mV depolarization of its membrane potential. Since these lenses have an input resistance of about 10 kohms, the total current associated with the pump can be estimated to be about 1 microampere. Since 1/2 of the Na-K ATPase is associated with the epithelial cells (Kinoshita, 1963), 0.5 microamps of the current should be produced by these cells. The area of the anterior surface of the lens with a 0.15 cm radius is about 0.15 cm^2. If each cell is 15 microns, by 15 microns, by 5 microns, the total number of epithelial cells should be about 7×10^4. The current per cell should then be about 7.5 pA. The power spectral density of the pump current noise with the pump modeled as a shot process is $Sp = 2qi(p)$ where q = elementary charge on an electron and $i(p)$ = the mean pump current. For a large cell with 10 pA mean pump current $Sp = 3.2 \times 10^{-30}$ Amp^2/Hz. In order to be able to see this current, the fluctuations must be greater than the competing irrelevant noise sources. The power spectral density of the Johnson (thermal) noise of the cell membrane is $4kT/R_m$ where k = Boltzmann's constant, T = absolute temperature, and R_m = the input resistance of the cell. For the 10 kohm-cm^2 membrane resis-

tance which we believe this cell has, the input resistance is 1.3×10^9 ohms. The minimum current noise that this membrane could produce is the Johnson noise whose power spectral density would be $S_m = 1.2 \times 10^{-29}$ Amp^2/Hz. In addition to this thermal noise, there would be a great deal of Lorentzian noise due to channels opening and closing. It is not possible to predict the amplitude of this noise component without knowing the conductance, the total number and the kinetics of the channels involved but it is certain that the noise would be large in comparison to the pump. This noise would have to be reduced substantially by blocking the channels. Since the dominant channel type should be a potassium channel for which there are many known blockers, this reduction may be possible. If we say that after such a block the resistance of the membrane increases 10 times, then the power spectral density of the membrane thermal noise under these conditions would be 1.2×10^{-30} Amp^2/Hz. Therefore, the total noise due to pump and membrane thermal noise is 4.4×10^{-30} Amp^2/Hz at low frequencies. Since the pump often moves 3Na/2K, the power spectrum should rise from the 4.4×10^{-30} Amp^2/Hz at low frequencies where fluctuations due to only the single net charge moved can be resolved to 5 times the low frequency power spectral density of the pump specific component at frequencies where the movement of all five charges can be resolved, to reach a final power spectral density of 1.7×10^{-29} Amp^2/Hz (membrane thermal noise + 5 times the low frequency pump noise). The corner frequency of this inverted Lorentzian spectrum should be related to the translocation time of the pump. Since a single cycle of the pump uses 1 ATP and since the ATP turnover rate is expected to be in the range of 50–150 ATP's/s (Hoffman, et al. 1979; Harms and Wright, 1980), a 1–300 Hz bandwidth should be adequate to resolve the important power spectrum of the pump.

It is unlikely that the PSD of the pump current can be measured to significantly higher frequencies than this. The resistance of the microelectrode in series with the capacitance of the cell is a noise source. The power spectral density of this noise should be described by $Se = 16pi^2kTR_eC_m{}^2f^2$ where k = Boltzmann's constant, T = absolute temperature, R_e = electrode resistance, C_m = membrane capacitance and f = frequency. For a 2 mohm electrode which is the largest we have been able to seal to these cells, and with an epithelial cell capacitance = 7.5 pF, the noise from this source would equal the pump noise at 475 Hz. It should be possible to enhance the quantitation of the pump-specific component by measuring the difference spectrum with and without ouabain. Even with the ionic conductances blocked, the pump could be expected to continue operation if the bath contained sufficient K and the electrode contained sufficient Na and ATP. Since the lumen of the pipette is in direct communication with the cell and since the volume of the pipette is considerably larger than that of the cell, the cellular concentrations of Na, K, and ATP would be those in the pipette. Sodium levels in the electrode could be selected to support a wide variety of pumping rates.

Thus, because of the wide variety of important information possible, it would seem worth the effort to work out the techniques to allow successful whole cell recording from epithelial cells.

It was not clear to us at the outset what time behavior to expect from epithelial channels. Would the channels be open at all times or would they open and close in a stochastic way similar to channels from excitable membranes? If they were always open, they could not be studied with the patch clamp unless substances could be found that would cause transient block of the channels. If they were always open, it would mean that the gross conductances of the cell were simply determined by the relative occurrence of the specific channel types (Na, K, Cl, etc.). On the other hand, if the channels opened and closed 'naturally', then the conductances of the cell would depend on the probability of the channels being open as well as the density of the various channel types. The early ensemble noise data available (Lindemann and Van Driessche, 1977; Van Driessche and Gogelein, 1978) led us to believe that the channels were naturally opening and closing and thus would be seen in the patch clamp as a stochastic stream of rectangular current pulses. In short, our initial measurement showed that this notion was correct in an extreme sense since it was immediately obvious that lens epithelium has a bewildering array of channels which show very rapid and complex time behavior. Some of the channels are obviously controlled by voltage and/or Ca.

Since we began this work, there have been at least three reports of single channel currents measured from epithelia. Maruyamu and Peterson (1983) reported channels from acinar cells of the pancreas which were quite similar to the non-selective cation channels reported from other tissues (Colquhoun et al., 1981; Yellen, 1982). Later, Maruyama et al. (1983) showed that isolated salivary gland cells possessed the Ca-activated K channels that had also been seen in other tissues (Marty, 1981; Pallotta et al., 1981). Recently, Sauve and coworkers (1983) have reported two K channels of 27 and 40 pS in Hela cells which to our knowledge have not been reported from other cells. Thus it is clear from the very beginning of this work that epithelia will have some channels common to those found in excitable cells but will also have some which may be specific to epithelia.

Our studies to date have concentrated on the apical membrane of lens epithelial cells from a number of species. Since it is known that most epithelial cells have different channel populations on their apical and basolateral surfaces, there is no reason to believe that we have yet sampled adequately all the channels which exist in our cells. At the present time, we have seen 11 different types of channels from the apical membrane alone. We call the channels different if their single channel conductances differ, their current-voltage relationships differ, or their selectivities differ. We have not yet carefully characterized the voltage dependence or kinetics of all of these channel types and thus within the population we have already seen, there may be more than 11 types when these parameters are considered.

In this section we will briefly describe this somewhat awesome number of channels so that the reader can appreciate, in general, what can be expected from epithelial patch clamping. More detailed accounts of the channels will be published elsewhere. In our earliest studies from *Rana pipiens* lens epithelium, we saw 6 channel types. The most common of these is a 25–30 pS channel which shows essentially perfect cation

selectivity over anions but does not select between Na and K (Fig. 6). This channel apparently occurs in clusters, with 3–5 being the usual number present in a patch if they are present at all. The probability of a channel being open depends on internal Ca and the time behavior of the channel is complex showing a very large number of rapid flickers per burst. This channel appears very similar to the non-selective cation channel reported by others although our channel shows somewhat more extensive flickering behavior than previously reported, perhaps due to the higher bandwidth and somewhat lower background noise of our recordings.

The second most common channel is a 50 pS channel whose selectivity for Na over K is about 1.2–1.8 (Fig. 7). This channel also seems to occur in clusters since whenever we see it, there is always more than one but in many patches the channel is absent. It is rare to see both the 25 pS and 50 pS channel in the same patch.

We have also seen a 100 pS non-selective cation channel whose reversal potential in excised patches is about zero mV with large Na, K, or Cl gradients across the channel (Fig. 8).

On rare occasions, we see a 40 pS channel that is nearly perfectly K-selective (Fig. 9). This channel has properties similar to the 40 pS K channel from Hela cells (Sauve et al., 1983) and perhaps is a channel which should be anticipated for other epithelia. We have seen it too infrequently to have a careful characterization of its properties.

Also on rare occasions, we have seen a 12 pS channel from *Rana pipiens* apical lens epithelial membrane (Fig. 10). This is a sodium-selective channel as judged by the reversal potential of its current. It is not anticipated that this is an amiloride sensitive channel since the impedance of the lens has no amiloride-sensitive component (Rae, unpublished observation).

Finally, the frog epithelium also contains a 4 pS channel whose extrapolated reversal

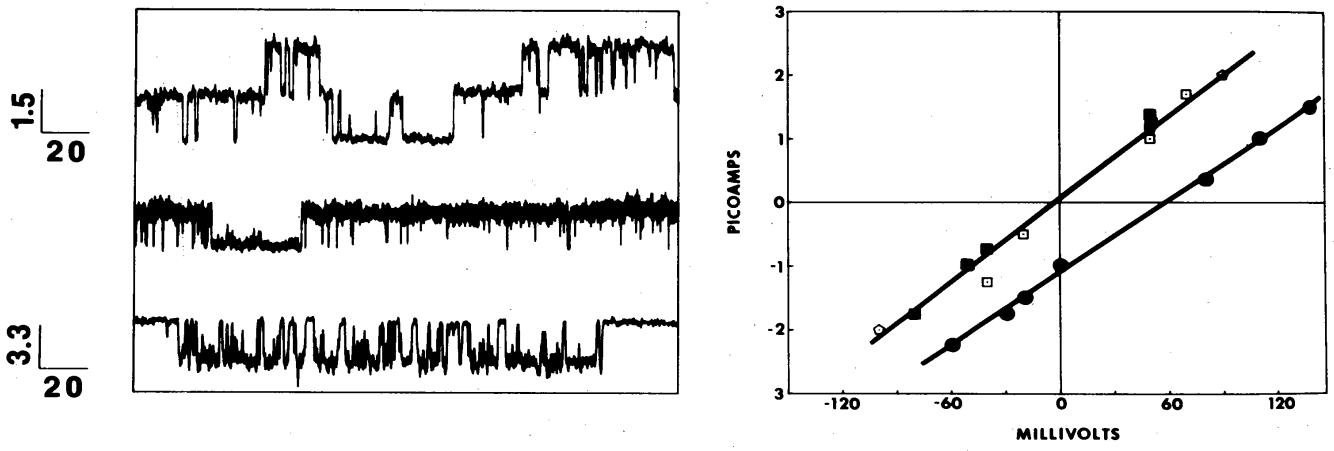

Fig. 6. 25 pS non-selective cation channel. Currents from single channels in the apical membrane of *Rana pipiens* lens epithelium. The top and bottom time records are from on-cell patches with 110 mM NaCl Ringer in the pipette. Middle time record is from inside-out patch with Ringer in pipette and 110 mM NaCl, 1 mM CaC12 Ringer in bath, a situation in which closure of the channel as shown is unusual. (●) Data are for an on-cell patch with 110 mM NaCl Ringer in the pipette. The remaining IV data are from an inside-out patch with (■) 110 mM NaCl Ringer on both sides, (□) 110 mM KCl Ringer in pipette, 110 mM NaCl Ringer in bath, (◈) 110 mM $NaMeSO_4$ Ringer in pipette, 110 mM NaCl Ringer in bath. Bandwidth = 2 kHz (8 pole Bessel filter). Corning #1723 glass. Voltages referred to cell interior. Calibration bars are in units of pA vertical scale and ms horizontal scale.

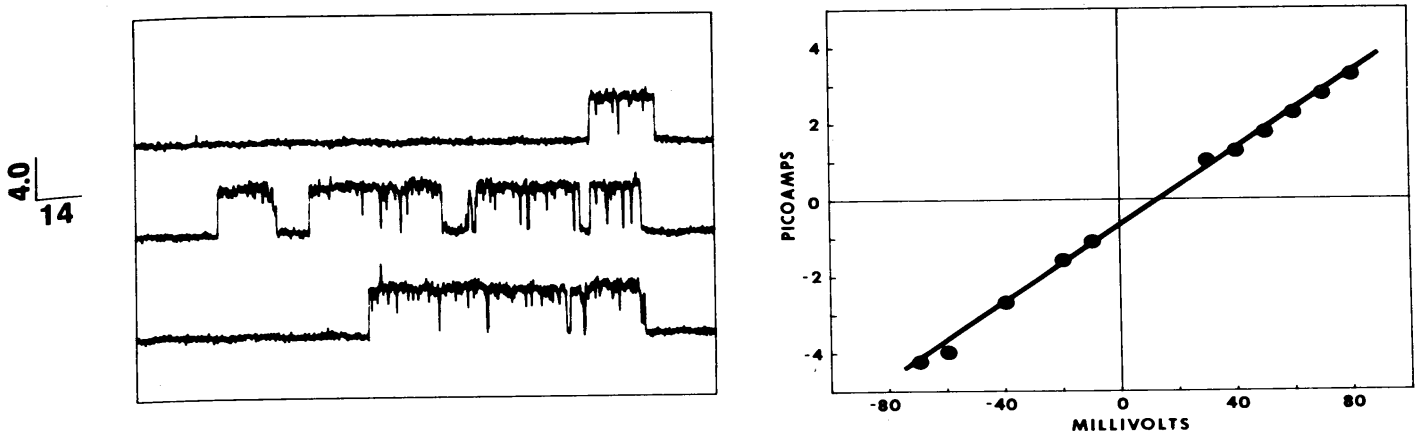

Fig. 7. 50 pS non-selective cation channel. Current from single channels in the apical membrane of *Rana pipiens* lens epithelium. IV data are from an inside-out patch with 110 mM NaCl Ringer in the pipette, 110 mM KCl Ringer in the bath. (Ek = –95 mV). Bandwidth = 3.5 kHz (8 pole Bessel filter). Corning #1723 glass. Voltage referred to cell interior. Calibration bars are in units of pA vertical scale and ms horizontal scale.

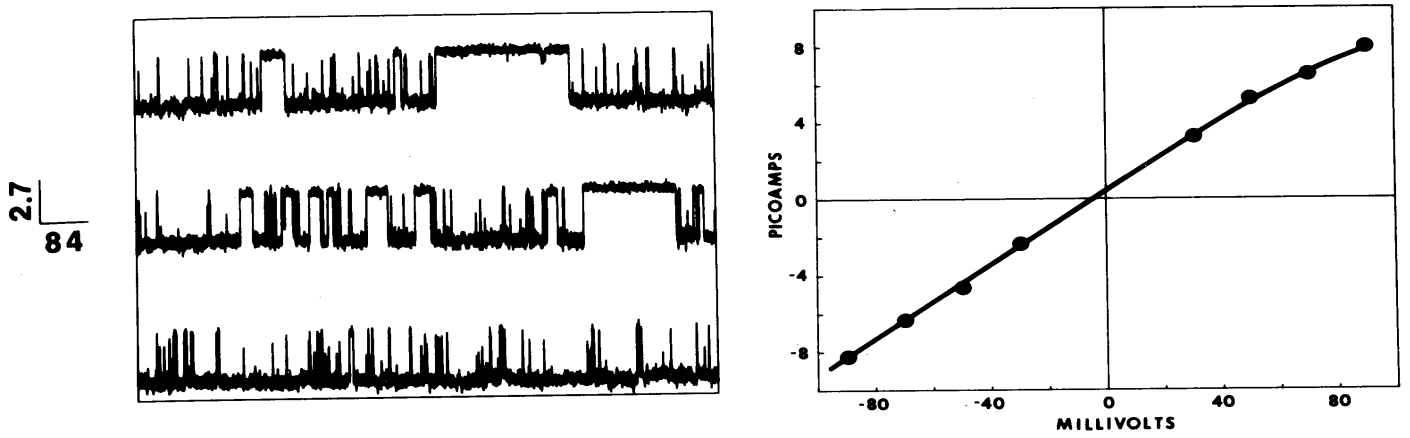

Fig. 8. 100 ps non-selective cation channel. Currents from single channels in the apical membrane of bullfrog lens epithelium. Data are from an inside-out patch with 100 mM KCl Ringer in the pipette and 110 mM NaCl Ringer in the bath. (Ek = 95 mV). Bandwidth = 2kHz (8 pole Bessel filter). Corning #7052 glass. Voltages referred to cell interior. Calibration bars are in units of pA vertical scale and ms horizontal scale.

potential is that expected for a Ca channel if the cell has an intracellular Ca concentration of 10^{-7} M. This channel is rare and difficult to resolve.

In the bullfrog, 12 pS, 25 pS, 50 pS, and 100 pS channels are also seen and are very similar to those seen in the small frog.

The epithelium of the mouse and the rat have channels similar to the 25 pS and 50 pS channels of the frog except their conductance is about 30 pS and 60 pS, respectively. This increase in conductance is about what would be anticipated for the more highly concentrated bathing solution of mammals in comparison to that for amphibians. There is also a 100 pS channel in these mammals but it is not yet clear that it is the same as that found in the amphibians. The mammals, however, have an amazing channel which we have seen in the bullfrog and grass frog on occasion, but which occurs

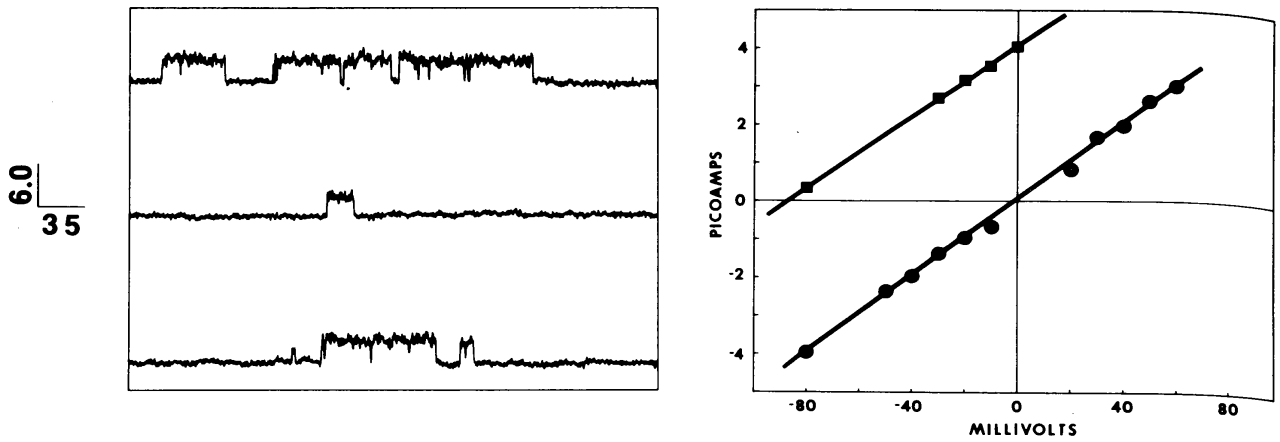

Fig. 9. 40 pS potassium channel. Currents from single channels in the apical membrane of *Rana pipiens* lens epithelium. (●) Data are for on-cell patch with 110 mM NaCl Ringer in pipette. (■) Data are for inside-out patch with 110 mM NaCl Ringer in pipette and 110 mM KCl Ringer in bath (Ek = −95 mV). Bandwidth = 1kHz (8 pole Bessel filter). Corning #7052 glass. Voltages referred to cell interior. Calibration bars are in units of pA vertical scale and ms horizontal scale.

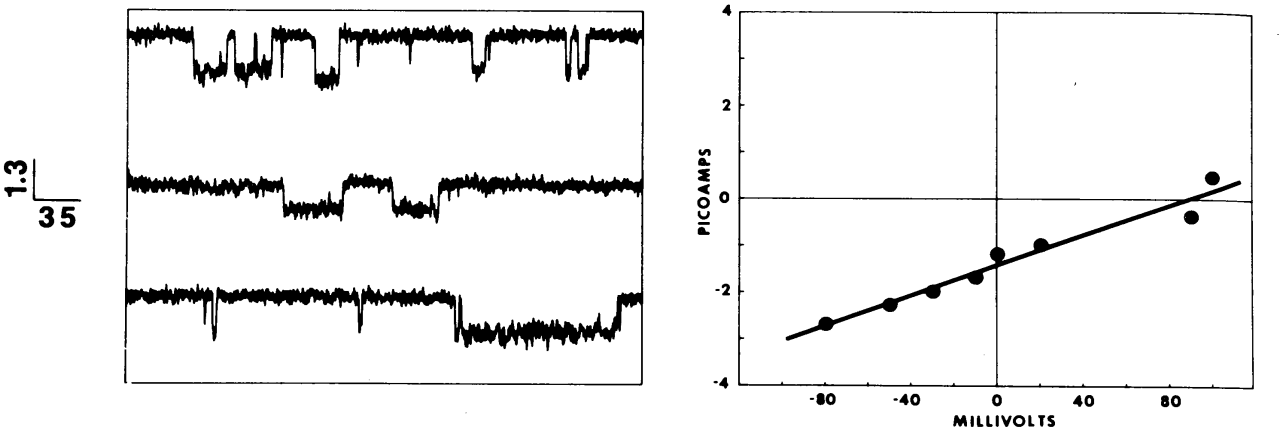

Fig. 10. 12 pS sodium channel. Currents from single channels in apical membrane of *Rana pipiens* lens epithelium. Data are from an inside-out patch with 110 mM NaCl Ringer in the pipette and 110 mM KCl Ringer in the bath. (ENa = 95 mV). Bandwidth = 1.5 kHz (8 pole Bessel filter). Corning #1723 glass. Voltages referred to cell interior. Calibration bars are in units of pA vertical scale and ms horizontal scale.

frequently in the mammals, particularly in the mouse lens epithelium (Fig. 11). A similar channel has also been seen in the corneal endothelium of the grass frog and the mouse. This is a giant channel which has an apparent conductance which varies between 400 pS and 1.9 nS from patch to patch. It is not unusual to be able to record currents of 100 pA through this channel. Based on its reversal potential in excised patches with Na, K, or Cl gradients across the patch, the channel has no selectivity for anions or cations. It does not appear to be the same as the large channel recently reported by Blatz and Magleby (1983) which is primarily anion-selective. The time behavior of the channel is the most complex we have observed. When the channel occurs in its minimum conductance configuration of around 400 pS, it appears to have 6 equal subconductance levels any of which it can enter stably for many milliseconds at a time. This channel flickers at an enormous rate with many flickers being unresolv-

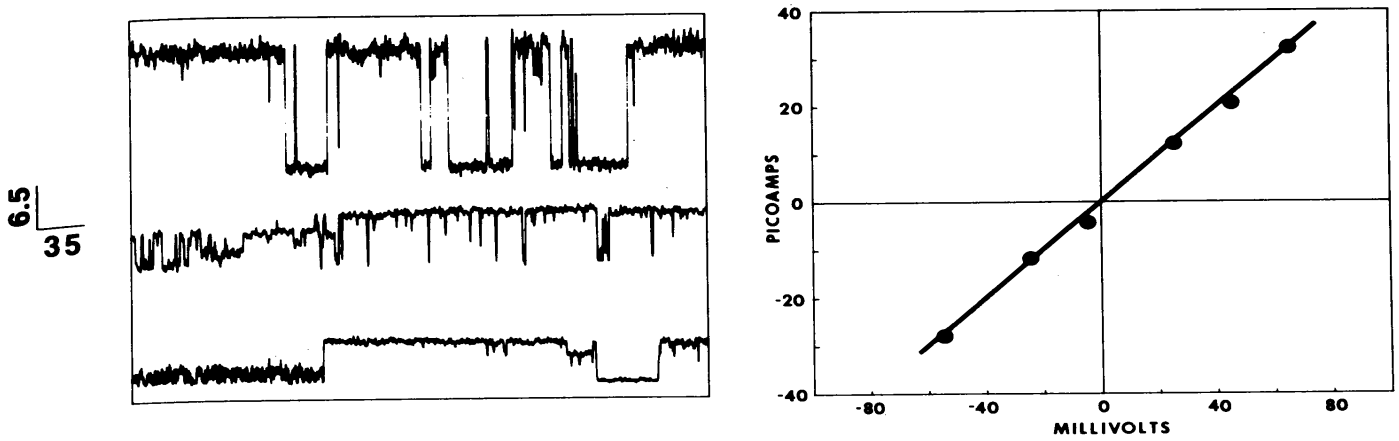

Fig. 11. 440 pS–1.9 nS non-selective channel. Currents from single channels in apical membrane of mouse lens epithelium (upper trace), bullfrog lens epithelium (middle trace) and mouse corneal endothelium (lower trace). IV data are from mouse inside-out lens epithelial patch with 150 mM KCl Ringer in pipette and 150 mM NaMeSO4 Ringer in bath. Bandwidth = 2 kHz (8 pole Bessel filter). Corning #7052 glass. Voltages referred to cell interior. Calibration bars are in units of pA vertical scale and ms horizontal scale.

ed even if the recordings are obtained at 30 kHz bandwidth. We do not believe that this is a membrane channel in the usual sense since the channel rarely occurs unless an externally applied field in excess of ± 70 mV is maintained across the patch for a minute or two. Since its conductance varies considerably from patch to patch in multiples of about 100 pS, it may not be a single channel but rather a parallel arrangement of 100 pS channels cooperatively gated. It does not seem possible that it is a parallel array of independently gated channels since, for example, the 'channel' frequently enters a regime where there are many closures from the apparent full open state to the full closed state, such simultaneous switching of independent channels being highly improbable if they are independently gated. The channel does not have the sensitivity to Ca or H^+ expected for junctional channels nor is it affected by antibodies to lens gap junctions or by calmodulin. However, these data do not rule out the possibility that it is a gap junction protochannel. Thus, its function is not clear although its occurrence is ubiquitous.

The lens epithelium of the chick has proven to be a rich source of channels. To date we have seen a 12 pS Na channel from the apical membrane of these cells as well as a 50 pS channel which shows only slight selectivity for Na over K. These channels seem similar to those seen in the amphibian epithelium. In addition, we have seen 5 different channels that are selective for potassium. There is a 45 pS channel and a 27 pS (Fig. 12) channel which are highly K selective and perhaps similar to those reported from Hela cells (Sauve et al., 1983). These often occur in the same patch, again similar to the finding from Hela cells. There are two large conductance K channels which are both activated by Ca, exhibit multiple subconductance levels, and have quite nonlinear current–voltage relationships when there is a substantial K gradient across the channel. Their slope conductances determined near their reversal potentials with symmetrical K solutions on both sides are 130 (Fig. 13) and 230 (Fig. 14) pS, respectively. The 130 pS K channel occurs at sufficient density that at least two such channels are found in almost every patch from the chick that we have examined. There is an 80 pS K

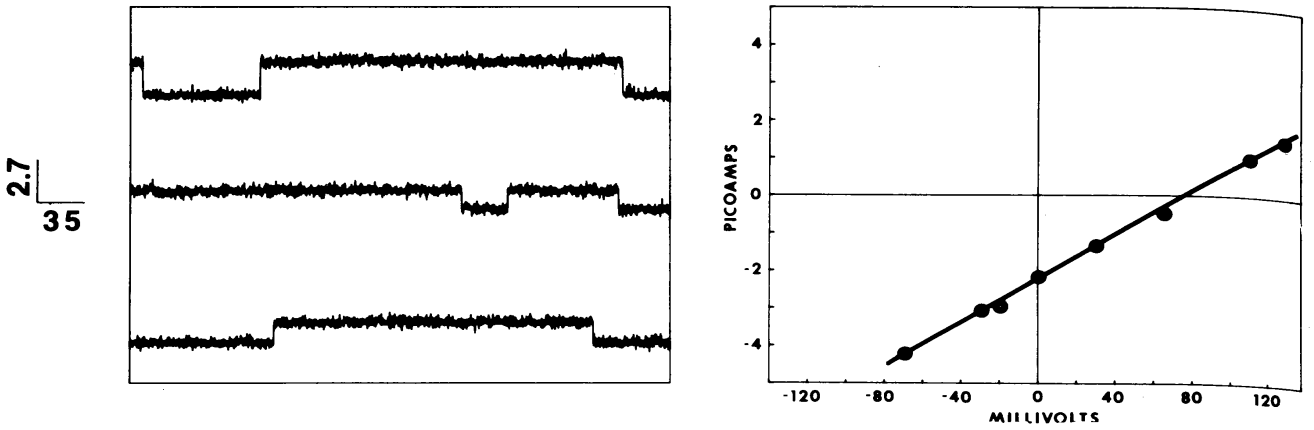

Fig. 12. 27 pS potassium channel. Currents from single K channels in apical membrane of chick lens epithelium. Data are from an inside-out patch with 150 mM KCl Ringer in pipette and 150 mM NaCl Ringer in bath. (Ek = 88 mV). Bandwidth is 2 kHz (8 pole Bessel filter). Corning #7040 glass. Caibration bars are in units of pA vertical scale and ms horizontal scale.

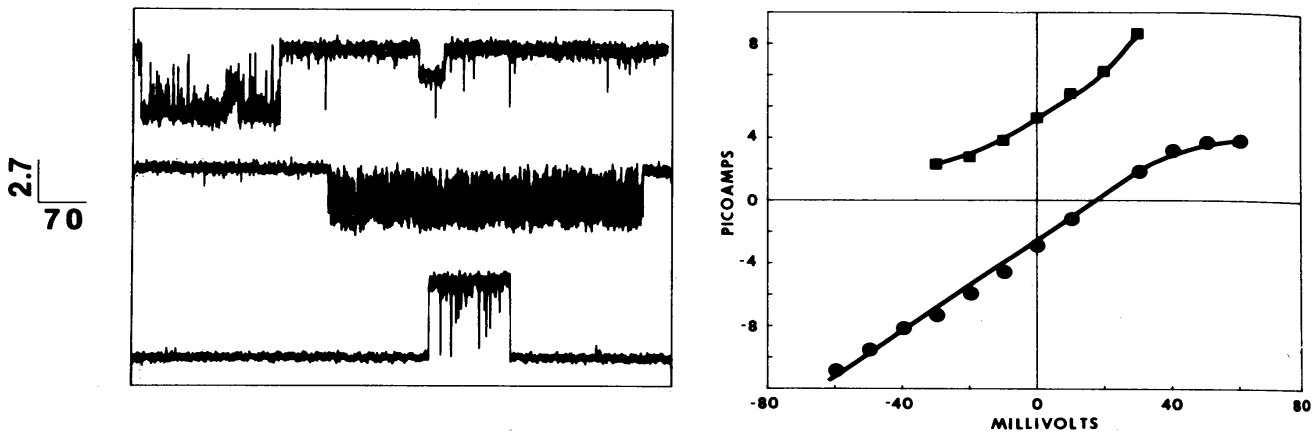

Fig. 13. 130 pS potassium channel. Currents from single K channels in the apical membrane of chick lens epithelium. Upper trace shows subconductance levels. Middle trace shows rapid flickering with 100 mM CsCl Ringer in pipette (on-cell patch). (●) Data are from on-cell patch with 150 mM KCl Ringer in pipette. (■) Data are from inside-out patch with 150 mM Ringer in pipette and 150 mM KCl Ringer in bath (Ek = −88 mV). Bandwidth = 2 kHz (8 pole Bessel filter). Corning #7052 glass. Voltages referred to cell interior. Calibration bars are in units of pA vertical scale and ms horizontal scale.

channel which is one of the simplest channels we have seen, in that it does not flicker at a high rate under recording conditions used to date (Fig. 15).

With such an array of channels, none of which have known pharmacology, it is likely to be some time before each channel is completely characterized. Some of the channels have quite linear current–voltage relationships. Some show rapid flickering and bursting behavior and we can anticipate that they have quite complex kinetics with numerous states being required to predict the time behavior of the channels in Markovian models. Some of the channels rectify, some show considerable voltage dependence, and some show clustered spatial distribution. Base on what we have seen so far, there is no reason to believe that epithelial channels will be less complex than those in excitable membranes. In fact, it is quite possible that the opposite is the case.

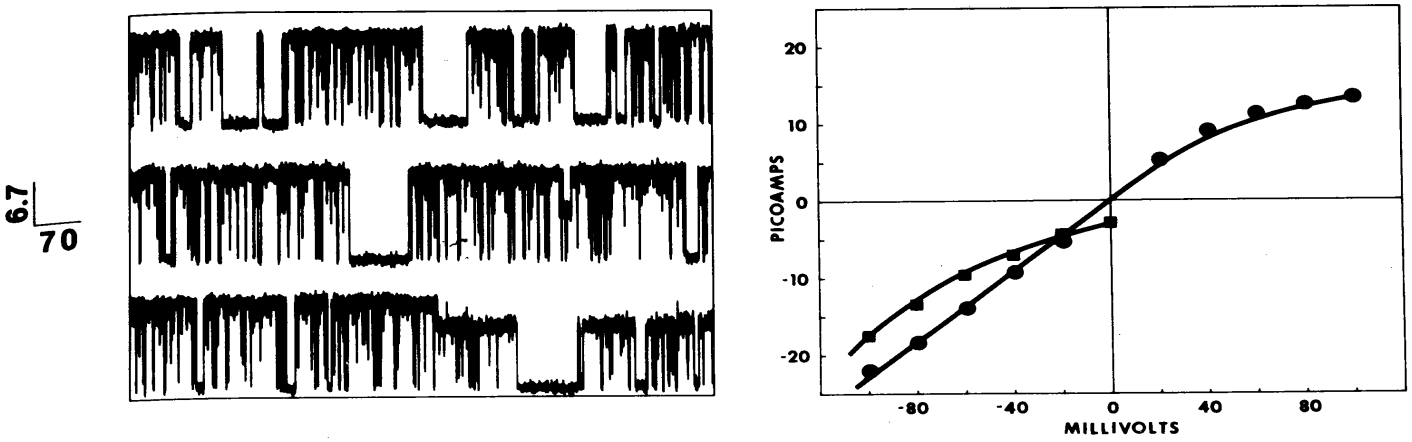

Fig. 14. 230 pS potassium channel. Currents from single K channels in apical membrane of chick lens epithelium. (●) Data are from on-cell patch with 150 mM KCl Ringer in pipette. (■) Data and time records are from the same patch inside-out with 150 mM NaCl Ringer in bath. (Ek = 88 mV). Bandwidth = 3 kHz (8 pole Bessel filter). Corning #7052 glass. Voltages referred to cell interior. Note subconductance levels. Calibration bars are in units of pA vertical scale and ms horizontal scale.

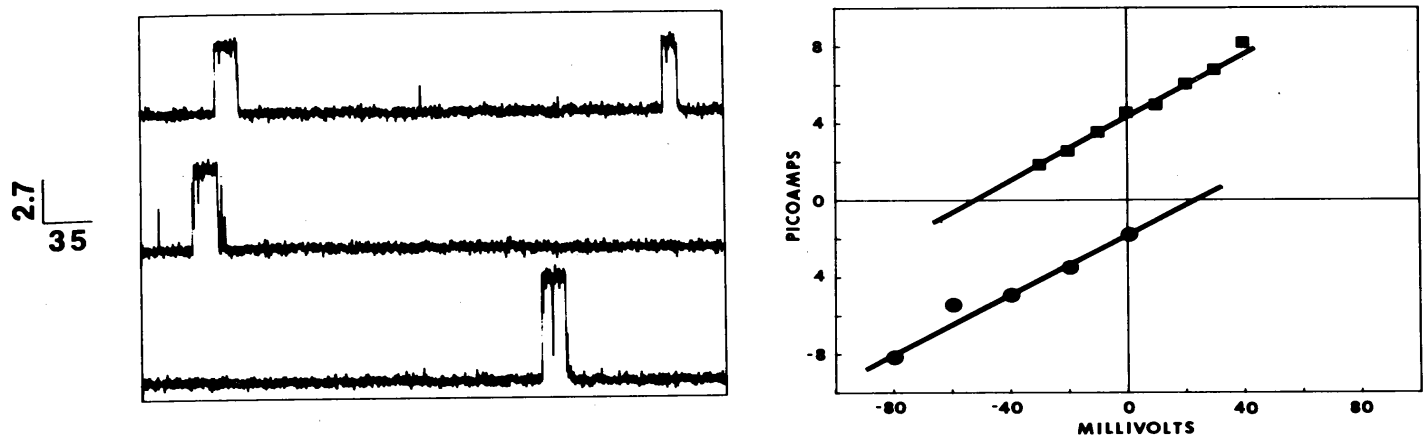

Fig. 15. 80 pS potassium channel. Currents from single channels in apical membrane of chick lens epithelium. (●) Data are from on-cell patch with 150 mM NaCl Ringer in pipette. (■) Data are from inside-out patch with 150 mM NaCl Ringer in pipette, 150 mM KCl Ringer in bath (Ek = −88 mV). Bandwidth = 2 kHz (8 pole Bessel filter). Corning #7052 glass. Voltages referred to cell interior. Calibration bars are in units of pA vertical scale and ms horizontal scale.

It also seems highly probable that many of the channels seen in the lens epithelium will turn out to be very similar to those seen in other epithelia. It is particularly perplexing that the density of channels and number of types of channels is so large since this was not predicted from our macroscopic measurements from the whole lens. We believe it will be some time before the microscopic measurements from the patch clamp can be reconciled with known macroscopic behavior from other measurements such as impedance or input resistance.

Improvements

There are several areas where improvements are required if patch clamping of epithelia and other tissues is to progress beyond its present capabilities. In general, there is a need for longer lasting, higher quality seals. With our cells, even though we are able to achieve a seal rate in excess of 90% of the attempts, it has been almost impossible to complete an optimal experimental protocol which involves multiple solution changes simply because of seal instability. In some preparations, just the ability to obtain seals consistently has been a problem. Both of these problems might be solved by further work in two areas. One, there is a need to develop techniques which clean extracellular matrix and debris from membrane surfaces without disrupting channel function. To our knowledge, this problem has not yet been studied systematically. Two, there is a need to develop better electrode materials which will seal more readily and interact more strongly with cell membranes. We have made some progress in this area with the use of specialty glasses on our cells, but there are many more glasses to be tested before these studies are completed.

At the present time, there is little improvement possible through better electronics since the best electronics presently available are not the limiting factor in noise performance and usable bandwidth. Although it would be better if the channels could be looked at with higher bandwidth recording and better signal to noise ratios, each of these advancements require higher resistance, lower noise seals, and better glasses. Since as previously stated, the noise of the seal and the noise of the glass are substantially greater than the noise of the electronics, the electronics are not really worth considerable additional effort until the glass and the seal problems are solved.

In the epithelium of the lens, there is the additional problem that the pharmacology of most of the channels is unknown. This problem coupled with the high channel density has made the detailed analysis of the kinetics of the channels difficult. In general, not only is there more than one channel in each patch, there is usually more than one kind of channel. While it is often possible to determine channel current–voltage relationships under these circumstances, analysis of kinetic states is almost impossible according to existing analysis schemes. There is a great need for specific channel blockers so that at least patches with only one kind of functioning channel can be obtained.

Usefulness of patch clamp with pitfalls

Regardless of the problems which presently exist with patch clamping, it is clear that it is extremely valuable when used in combination with other techniques. Patch clamping allows one to determine the conductance of the single channel, which by itself would be of sufficient value to justify use of the technique. While noise measurements can sometimes deal with the kinetics of multiple channels, the single channel conductances and kinetics which can be calculated by noise techniques depend on assumptions about which one cannot be certain. Noise analysis becomes a much more

powerful technique when the single channel conductances and some features of the underlying channel behavior (kinetics) are known.

Patch clamping also allows one to determine the selectivities of individual channels. Present measurements have shown that there is a population of channels in epithelial membranes which are quite non-selective or select only at the level of anions *vs* cations. Since in an optimally performed patch clamp situation, the cells from which the patch is taken are viewed directly in a compound microscope, it is possible to know precisely the location on the cell from which the patch came. This should be invaluable in sorting out the apical *vs* basolateral distribution of channels in epithelia.

The time record of the currents from single channels can be analyzed from the standpoint of probability that the channel will be open, the distribution of open times, and distribution of closed times. Such analyses provide information about the kinetic schemes which describe the rearrangement of the channel protein in going from closed to open states and back. Thus the patch clamp technique provides the most direct information at the molecular level concerning the mechanisms of action of channel proteins. Presently, these analyses are not totally satisfying since even from the more easily analyzed channels, the number of kinetic states needed to describe channel behavior is large (Barrett et al., 1982). Of course, it is also possible to use these techniques to understand the mechanism of action of specific drugs since many drugs act directly or indirectly at the level of the channel proteins to change channel kinetics, conductance or selectivity.

Using the procedure known as whole cell clamping in concert with ion substitutions (both inside the cell and outside), it is possible to characterize the macroscopic conductance of entire cells. Since this information is lacking for almost all epithelia, whole cell clamping is likely to be an important tool to epitheliology, particularly for isolated cells. Whole cell clamping can, of course, be used in concert with impedance techniques or noise techniques to more precisely characterize conductance and surface area properties of single cells.

As we described earlier, under favorable circumstances it might even be possible to directly characterize the current produced by pumps such as the Na-K pump present in most membranes. Pump current measurement will depend on the ability to find specific channel blockers, but in principle they are possible within the signal to noise level achievable with the whole cell clamp.

However, as promising as the patch clamp technique seems, it has some restrictions that merit discussion. For example, it is unlikely that the simple measurement of single channel currents will by itself greatly improve our knowledge of cell function. Precise measurements of macroscopic properties will be useful to make sense of single channel kinetics. This is perhaps analogous to understanding the individual logic gates in a computer which would appear only as a bewildering array of switches unless one knew at a higher level how the switching combined to produce higher level functions.

The role of the particular channels seen in the patch may be very difficult to determine. For example, it is possible that membranes contain a large number of proteins which are potentially channels not used by the intact cell, but under some circumstances might be measured in the patch clamp. For us, this concern arises from the fact that many of our patches have no apparent channels in them after the seal is

formed. However, after time and/or the application of large fields of voltage across the patch, channels often appear that were not obvious initially. Sometimes 'channelless' patches suddenly have many channels following the application of a little additional suction. These kinds of observations cause concern about the relevance of the channels seen under these circumstances.

It is also possible that the channels may be measured in circumstances where some vital control substances usually present inside the cell are lacking. This is of particular concern in the excised patch configurations. This is why it is very important to characterize the channels in on cell patches from healthy cells in addition to characterizing them off the cell. It is even possible that the channels are altered in some way by the patching procedure and again it is important to compare their characteristics determined from patches to those determined from macroscopic measurements.

Finally, the limited bandwidth of the technique may significantly distort the kinetics determined from patches. For example, in many of the channels we have seen from our cells, the flicker rate of the channel is fast relative to our recording bandwidth. This causes an error in the estimate of channel open and closed times. For channels with small single channel conductances and short open times, the signal to noise of the patch clamp may not allow even the detection of the channels. Certainly at the present time, 'fast' channels with a conductance of 1 pS or less would be very difficult to deal with in the patch clamp.

All in all, the usefulness of patch clamping would seem to far outweigh the problems even though some early caution would seem advisable. Thus one anticipates that an informed application of the technique to many cells will result in considerable new knowledge about channel proteins and their control and provide new insight into transport processes.

Acknowledgements

We wish to thank R.S. Eisenberg and R.T. Mathias for carefully reading the manuscript and making many useful suggestions. We also wish to thank F. Sigworth for kindly providing the National Micronetics feedback resistor used in our headstage amplifier and for many useful discussions over the past several years. The work was supported by grants EY03282 and RR05477 from the National Institutes of Health, the Regenstein Foundation, and the Louise C. Norton Trust.

References

Auerbach, A. and Sachs, F. (1983): Flickering of a nicotinic ion channel to a subconductance state. Biophys. J. 42, 1–10.

Axelrod, D. (1981): Zero-cost modification of bright field microscopes for imaging phase gradient on cells: schlieren optics. Cell Biophysics 3, 167–173.

Bacigalupo, J. and Lisman, J.E. (1983): Single-channel currents activated by light in Limulus ventral photoreceptors. Nature 304, 268–270.

Barrett, J.N., Magleby, K.L. and Pallotta, B.S. (1982): Properties of single calcium-activated potassium channels in cultured rat muscle. J. Physiol. 331, 211–230.

Blatz, A.L. and Magleby, K.L. (1983): Single voltage-dependent chloride-selective channels of large conductance in cultured rat muscle. Biophys. J. 43, 237–241.

Brown, A.M., Camerer, H., Kunze, D.L. and Lux, H.D. (1982): Similarity of unitary Ca^{2+} currents in three different species. Nature 299, 156–158.

Cachelin, A.B., De Payer, J.E., Kokubun, S. and Reuter, H. (1983): Ca^{2+} channel modulation by 8-bromo-cyclic AMP in cultured heart cells. Nature, 304, 462–464.

Clark, R.N. (1964): Introduction to Automatic Control Systems. Wiley, New York.

Colquhoun, D. and Hawkes, A.G. (1981): On the stochastic properties of single ion channels. Proc. R. Soc. Lond., B211, 205–235.

Colquhoun, D. and Hawkes, A.G. (1982): On the stochastic properties of bursts of single ion channel openings and of clusters of bursts. Phil. Trans. R. Soc. Lond., B300, 1–59.

Colquhoun, D., Neher, E., Reuter, H. and Stevens, C.F. (1981): Inward current channels activated by intracellular Ca in cultured cardiac cells. Nature 294, 752–754.

Conti, F. and Neher, E. (1980): Single channel recordings of K^+ currents in squid axons. Nature 285 (5761), 140–143.

Corey, D.P. and Stevens, C.F. (1983): Science and Technology of Patch-Recording Electrodes in Single Channel Recording (Sakmann and Neher, eds.) Plenum, New York.

Cull-Candy, S.G., Miledi, R. and Parker, I. (1980): Single glutamate-activated channels recorded from locust muscle fibres with perfused patch-clamp electrodes. J. Physiol., 321, 195–210.

DeFelice, L.J. and Firth, D.R. (1971): Spontaneous voltage fluctuations in glass microelectrodes. IEEE Trans. Biomed. Eng., BME-18, 339–351.

Dionne, V.E. and Leibowitz, M.D. (1982): Acetylcholine Receptor Kinetics. A description from single channel currents at snake neuromuscular junction. Biophys. J., 39, 253–261.

Dostal, J. (1981): Operational Amplifiers. Elsevier, Amsterdam.

Evans, A.D., editor (1981): Designing with Field-Effect Transistors. McGraw-Hill, New York.

Fenwick, E.M., Marty, A. and Neher, E. (1982): A patch-clamp study of bovine chromaffin cells and of their sensitivity to acetylcholine. J. Physiol., 331, 577–597.

Fenwick, E.M., Marty, A. and Neher, E. (1982): Sodium and calcium channels in bovine chromaffin cells. J. Physiol., 331, 599–635.

Fishman, H.M. (1973): Relaxation spectra of potassium channel noise from squid axon membranes. Proc. Natl. Acad. Sci. U.S.A. 70 (3), 876–879.

FitzHugh, R. (1983): Statistical properties of the asymmetric random telegraph signal, with applications to single-channel analysis. Mathematical Biosciences 64, 75–89.

Fukushima, Y. (1981): Identification and kinetic properties of the current through a single Na^+ channel. Proc. Natl. Acad. Sci. U.S.A. 78 (2), 1274–1277.

Fukushima, Y. (1982): Blocking kinetics of the anomalous potassium rectifier of tunicate egg studied by single channel recording. J. Physiol., 331, 311–331.

Hamill, O.P., Marty, A., Neher, E., Sakmann, B. and Sigworth, F.J. (1981): Improved patch-clamp techniques for high-resolution current recording from cells and cell-free membrane patches. Pflugers Arch., 391, 85–100.

Hamill, O.P. and Sakmann, B. (1981): Multiple conductance states of single acetylcholine receptor channels in embryonic muscle cells. Nature 294, 462–466.

Harms, V. and Wright, E.M. (1980): Some characteristics of Na/K-ATPase from rat intestinal basal lateral membranes. J. Membr. Biol., 53, 119–128.

Hoffman, J.F., Kaplan, J.H. and Callahan, T.J. (1979): The Na:K pump in red cells is electrogenic. Fed. Proc., 38, 2440–2441.

Horn, R. (1984): Gating of channels in nerve and muscle a stochastic approach. In: Ion Channels: Molecular and Physiological Aspects (Stein, W.D., ed.) Academic Press, In press.

Horn, R. and Lange, K. (1983): Estimating kinetic constants from single channel data. Biophys. J., 43, 207–223.

Horn, R. and Patlak, J. (1980): Single channel currents from excised patches of muscle membrane. Proc. Natl. Acad. Sci. U.S.A. 77(11), 6930–6934.

Horn, R., Patlak, J. and Stevens, C.F. (1981): Sodium channels need not open before they inactivate. Nature 291, 426–427.

Horn, R., Patlak, J. and Stevens, C.F. (1981): The effect of tetramethylammonium on single sodium channel currents. Biophys. J.,6, 321–327.

Jung, W.G. (1980): IC Op Amp Cookbook. Howard W. Sams & Co., Inc., Indianapolis, IN.
Kinoshita, J.H. (1963): Selected topics in ophthalmic biochemistry. Arch. Ophthalmol., 70, 558–573.
Lee, K.S., Akaike, N. and Brown, A.M. (1978): Properties of internally perfused, voltaged-clamped, isolated nerve cell bodies. J. Gen. Physiol., 71, 489.
Levis, R.A. (1981): Patch and axial wire voltage clamp techniques and impedance measurements from cardiac Purkinje fibers. Ph.D. Thesis, University of California, Los Angeles.
Lindemann, B. (1980): The beginning of fluctuation analysis of epithelial ion transport. J. Membr. Biol., 54, 1–11.
Lindemann, B. and Van Driessche, W. (1977): Sodium-specific membrane channels of frog skin are pores: current fluctuations reveal high turnover. Science 195, 292–294.
Lux, H.D., Neher, E. and Marty, A. (1981): Single channel activity associated with the calcium-dependent outward current in Helix pomatia. Pflugers Arch. 389, 293–295.
Marty, A. (1981): Ca-dependent K channels with large unitary conductance in chromaffin cell membranes. Nature 291, 497–500.
Maruyama, Y., Gallacher, D.V. and Petersen, O.H. (1983): Voltage and Ca^{2+}-activated K^+ channel in basolateral acinar cell membranes of mammalian salivary glands. Nature 302, 827–829.
Maruyama, Y. and Petersen, O.H. (1982): Single-channel currents in isolated patches of plasma membrane from basal surface of pancreatic acini. Nature, 299, 159–161.
Motchenbacher, C.D. and Fitchen, F.C. (1973): Low Noise Electronic Design. Wiley, New York.
Neher, E. (1981): Unit conductance studies in biological membranes. In: Techniques in Cellular Physiology (Baker, P.F., ed.) Elsevier, Amsterdam.
Neher, E. and Sakmann, B. (1976): Single-channel currents recorded from membrane of denervated frog muscle fibres. Nature 260, 799–802.
Neher, E., Sakmann, B. and Steinbach, J.H. (1978): The extracellular patch clamp: a method for resolving currents through individual open channels in biological membranes. Pflugers Arch., 375, 219–228.
Neher, E. and Steinbach, J.H. (1978): Local anaesthetics transiently block currents through single acetylcholine-receptor channels. J. Physiol., 277, 153–176.
Nelson, D.J. and Sachs, F. (1979): Single ionic channels observed in tissue-cultured muscle. Nature 282 (5741), 861–863.
Netzer, Y. (1981): The design of low-noise amplifiers. Proc. IEEE, 69, 728–741.
Noma, A. (1983): ATP-regulated K^+ channels in cardiac muscle. Nature 305, 147–148.
Pallotta, B.S., Magleby, K.L. and Barrett, J.N. (1981): Single channel recordings of Ca^+-activated K^+ currents in rat muscle cell culture. Nature 293, 471–474.
Patlak, J.B., Gration, K.A.F. and Usherwood, P.N.R. (1979): Single glutamate-activated channels in locust muscle. Nature 278, 643–645.
Rae, J.L. and Levis, R.A. (1984): Patch clamp recordings from the epithelium of the lens obtained using glasses selected for low noise and improved sealing properties. Biophys. J., 45, 144–146.
Reuter, H., Stevens, C.F., Tsien, R.W. and Yellen, G. (1982): Properties of single calcium channels in cardiac cell culture. Nature 297, 501–504.
Sachs, F. and Neher, E. (1983): In Single Channel Recordings, (Sakmann and Neher, eds.) Plenum, New York.
Sachs, F., Neil, J. and Barkakati, N. (1982): The automated analysis of data from single ionic channels. Pflugers Arch., 395, 331–340.
Sakmann, B. and Neher, E. (1983): Single Channel Recording. Plenum, New York.
Sauvé, R., Roy, G. and Payet, D. (1983): Single channel K^+ currents from HeLa cells. J. Membr. Biol., 74, 41–49.
Siegelbaum, S.A., Camardo, J.S. and Kandel, E.R. (1982): Serotonin and cyclic AMP close single K^+ channels in aplysia sensory neurones. Nature 299, 413–417.
Sigworth, F.J. (1983): Electronic design of the patch clamp. Single Channel Recordings, (Sakmann and Neher, eds.) Plenum, New York.
Sigworth, F.J. and Neher, E. (1980): Single Na^+ channel currents observed in cultured rat muscle cells. Nature 287, 447–449.
Tobey, G.E., Graeme, J.G. and Huelsman, L.P. (1971): Operational Amplifiers Design and Applications. McGraw Hill, New York.

Valdiosera, R., Clausen, C. and Eisenberg, R.S. (1974): Measurement of the impedance of frog skeletal muscle fibers. Biophys. J., 14(4), 295–315.

Van der Ziel, A. (1962): Thermal noise in field effect transistors. Proc. IEEE, 50, 1808–1812.

Van der Ziel, A. (1963): Gate noise in field effect transistors at moderately high frequencies. Proc. IEEE, 51, 461–467.

Van Driessche, W. and Gogelein, H. (1978): Potassium channels in the apical membrane of the toad gall-bladder. Nature 275, 665–669.

Van Driessche, W. and Zeiske, W. (1980): Ba^{2+}-induced conductance fluctuations of spontaneously fluctuating K^+ channels in the apical membrane of frog skin (*Rana temporaria*). J. Membrane Biol., 56, 31–42.

Van Driessche, W. and Zeiske, W. (1980): Spontaneous fluctuations of potassium channels in the apical membrane of frog skin. J. Physiol., 299, 101–116.

Wong, B.S., Lecart, H. and Adler, M. (1982): Single calcium-dependent potassium channels in clonal anterior pituitary cells. Biophys. J. 39, 313–317.

Yellen, G. (1982): Single Ca^{2+}-activated nonselective cation channels in neuroblastoma. Nature 296, 357–359.

Zeiske, W. and Van Driessche, W. (1981): Apical K^+ channels in frog skin (*Rana temporaria*): cation adsorption and voltage influence gating kinetics. Pflugers Arch., 390, 22–29.